

Positron Emission Tomography Imaging of Regional Cerebral Glucose Metabolism

Abass Alavi, Robert Dann, John Chawluk, Jane Alavi, Michael Kushner, and Martin Reivich

The (¹⁸F) fluorodeoxyglucose (FDG) technique to measure local cerebral metabolic rate for glucose (LCMR_{Glu}) is well accepted and widely used by many institutions around the world. A large number of studies has been carried out in normal volunteers and patients with a variety of CNS disorders. Several investigators have noted that no significant age-related changes in cerebral glucose use occur with normal aging. Some important and interesting findings have been revealed following sensory, motor, visual, and auditory stimulations. Functional imaging with FDG in certain neurologic disorders has dramatically improved our understanding of their underlying pathophysiologic phenomena. Some abnormalities detected on the positron emission tomography (PET) images have no corresponding changes on either x-ray computed tomograms (XCT) or magnetic resonance images (MRI). In patients with Alzheimer's disease, primary sensorimotor, visual, and cerebellar metabolic activity appears relatively preserved. In contrast, parietal, temporal, and to some degree, frontal glucose metabolism is significantly diminished even in the early stages of the disease. Patients with Huntington's disease and those at risk of developing this disorder have a typical pattern of diminished CMR_{Glu} in the caudate nuclei and putamen. In patients with stroke, PET images with FDG have demonstrated abnormal findings earlier than

either XCT or MRI and with a wider topographic distribution. FDG scans have revealed interictal zones of decreased LCMR_{Glu} in approximately 70% of patients with partial epilepsy. The location of the area of hypometabolism corresponds to the site of the epileptic focus as determined by electroencephalography and microscopic examination of the resected tissue. Ictal scans during partial seizures demonstrate areas of hypometabolism corresponding to the sites of seizure onset and spread. Several investigators have reported relative hypofrontal CMR_{Glu} in patients with schizophrenia. In our center, FDG scans from patients with schizophrenia were successfully differentiated from those obtained in normal controls. Finally, our preliminary data (using PET, XCT, and MRI) in patients with CNS disorders indicate that MRI provides excellent delineation of the structural abnormalities. It may prove to be superior to XCT in the evaluation of certain diseases such as cerebral ischemia and infarcts, head injury, tumors, and white matter lesions. Metabolic imaging with FDG provides functional information not obtainable with either MRI or NMR spectroscopy. Therefore, PET studies will play a complementary role to the anatomic imaging in the management of patients with CNS disorders.

© 1986 by Grune & Stratton, Inc.

THE (¹⁸F) fluorodeoxyglucose (FDG) technique to measure local cerebral glucose metabolic rate (LCMR_{Glu}) is the extension into human studies of the autoradiographic (¹⁴C)-deoxyglucose (DG) technique developed by Sokoloff et al.¹ Both DG and FDG are transported between blood and brain by the same saturable carrier that transports glucose,² and both compete with glucose in the tissue for hexokinase, which phosphorylates them to their respective hexose-6-phosphates.³ In contrast with

glucose-6-phosphate, the deoxyglucose-6-phosphate is essentially trapped at this point and undergoes no further steps in the normal glycolytic pathway. This provides the basis for the DG and FDG measurement techniques, which use a kinetic model with measurable parameters (rate constants, lumped constant, arterial curve, plasma glucose, etc) to estimate the rate of glucose use during steady state conditions. For a detailed description of the model, assumptions, and methods used in both techniques, refer to the reports describing both DG and FDG,^{1,4-6} or to recent reviews of the techniques.^{7,8}

The DG technique has been used to study cerebral function and organization in a large number of animal species. The list of references using this method, if cited, would run into the thousands. With the invention of positron emission tomography (PET), it became possible to replace autoradiograms with *in vivo* images of the brain, thus allowing the DG technique to be applied to studies of man by labeling the DG with an appropriate positron-emitting radionu-

From the Division of Nuclear Medicine, Department of Radiology, Cerebrovascular Research Center, Department of Neurology, and Cancer Center, University of Pennsylvania School of Medicine, Philadelphia.

Supported by National Institutes of Health Grants No. NS 14867-01 and NIH AG 03934-01, and the Sandie Altman foundation.

Address reprint requests to Abass Alavi, MD, Division of Nuclear Medicine, Hospital of the University of Pennsylvania, 3400 Spruce St, Philadelphia, PA 19104.

© 1986 by Grune & Stratton, Inc.
0001-2998/86/1601-0001\$05.00/0

clide.⁹ Both C-11 and F-18 have been used successfully,^{7,8,10} with FDG being by far the more commonly used radiopharmaceutical. Since its inception, the PET-FDG technique has been used to study cerebral organization in the normal human brain, as well as to study disruptions of this organization produced in various disease states. Analysis of FDG images can be approached at two distinct levels. For clinically useful estimates of metabolism in patients, adequate diagnosis may be possible by using average values for the kinetic rate constants and the lumped constant.^{5,10} Indeed, tomographic images of a tumor, for example, may prove to be sufficient for diagnostic purposes even without quantitative metabolic data. However, the potential of PET techniques, including FDG, is far greater than this. They can be used, with appropriate modeling and quantitation, to explore the basic biochemical and physiologic mechanisms by which the human brain operates. To accomplish this requires more detailed examination of each step in the process of quantitation.

We and other groups have measured the kinetic rate constants in man,^{5,10,11} and in general have found very little difference in the mean values. When a group of young control subjects were analyzed using the constants we measured¹⁰ and with the constants reported by Phelps et al.,⁵ no significant difference was found between the two sets of data. In addition, the metabolic rates determined with both individual and group mean values did not differ significantly (Table 1). This would suggest that the use of average values in normal subjects introduces little or no error in metabolic calculations. The rate constants may change, however, with aging or within regions undergoing pathologic changes,^{12,13} so in order to accurately measure metabolism in these regions it may be necessary to determine the rate constants individually.

Common to all of the measurement techniques above is the so called lumped constant, which is basically a conversion factor between deoxyglucose and glucose. We have measured the lumped constant for both DG and FDG in young normal volunteers and found the mean values to be 0.56 ± 0.043 and 0.52 ± 0.028 , respectively.¹⁰ These are global values rather than regional, and are strictly applicable only to studies of normal subjects, and possibly of patients with diffuse

Table 1. Global Metabolic Rates Using FDG and the k4 Model

	Mean Rate Constants (Phelps et al ⁵)	Mean Rate Constants (Reivich et al ¹⁰)	Individual Rate Constants (Present report)
Control subjects*			
1	5.39	4.93	
2	6.87	6.52	
3	5.48	5.16	
4	5.36	5.10	
5	5.31	5.06	
6	8.98	8.55	
7	9.63	9.14	
8	7.12	6.70	
Rate constant subjects†			
1	6.74	6.36	6.86
2	7.75	7.31	7.03
3	5.12	4.81	4.75
4	8.41	7.93	7.76
5	4.62	4.38	4.60

*Mean: 6.77 ± 1.73 (A), 6.40 ± 1.67 (B).

†Mean: 6.53 ± 1.64 (C), 6.16 ± 1.54 (D), 6.20 ± 1.43 (E).

Note. Control subjects: (A) v (B): $t = 0.44$, $P > .6$. Rate constant subjects: (C) v (D): $t = 0.37$, $P > .6$; (D) v (E): $t = 0.04$, $P > .9$. Global metabolic rates were calculated using the k4 model and rate constants measured by Phelps et al.⁵ Reivich et al.¹⁰ and the individual constants used to generate the mean values reported by Reivich et al. Control subjects were studied in the eyes and ears closed state, while rate constant subjects were studied while undergoing a variety of different sensory stimulation paradigms. All subjects were young, normal right-handed men. A lumped constant of 0.52 was used for all calculations.

cerebral disease such as Alzheimer's disease, using radiopharmaceuticals produced by the same syntheses. The lumped constant may assume different values in pathologic states, as suggested by the work in rats of Crane et al.¹⁴ Regional estimates of the lumped constant have been made recently by Gjedde et al¹⁵ using (C-11) methylglucose. They found that the lumped constant varied insignificantly from region to region within the brain, was the same for gray and white matter, and did not differ between patients, although it was inversely proportional to metabolic rate. In recently infarcted regions, however, they found almost a ten-fold range (from 0.37 to 2.83) and were able to identify two distinct classes of infarcts, one with normal values and the other with lumped constants greater than unity.

The technical limitations of PET imaging have been described thoroughly in a series of articles by the University of California at Los Angeles (UCLA) group¹⁶⁻²² and include the effects of

spatial resolution of the tomograph, uniformity of resolution, counting statistics, scatter, random coincidences, attenuation correction, and physical-anatomical effects. Most recently, Hoffman et al²³ have noted that with FDG it is already possible to obtain measurement precision of 1% to 2% with several million counts per image. The resolution of the current generation of imaging devices is approaching the theoretic limit in humans of 2 to 3 mm, which will allow improvements in the accuracy of metabolic rate determinations as well.

The neuroscientist investigating the functional organization of animal brains has at his command a wide variety of tools to explore both anatomy and function, including anatomic tracing techniques based on axonal transport, single unit electrophysiology, and studies of behavior following cortical lesions or section of selected fibers. The DG technique can be used in conjunction with all of these to measure functional activity in anatomically defined structures, since cell or fiber stains of the tissue sections allow the determination of boundaries of Broadmann's areas.²⁴ In this way the functional map (autoradiogram) can be related unambiguously to the underlying anatomy.

The traditional view of cerebral organization has been that of a serial hierarchy of processing. A vast amount of anatomic and physiologic evidence in animals including primates, recently reviewed by Diamond²⁵ and Merzenich and Kaas,²⁶ suggests a more complex scheme of organization. There is a rich cortical interplay of parallel, serial, and recurrent components, involving both ipsilateral and contralateral corticocortical projections. For any given perception, thought, or behavior to occur, it is apparent that the integrated activity of a multitude of different neurons throughout the brain must be involved. Since each cortical area receives input from several other areas and sends projections to multiple regions, it may also serve multiple functions involving each of the neural circuits in which it is included. This complex organization must be considered by the investigator exploring human brains with the FDG technique. The design and interpretation of studies involving functional imaging take on added importance when one realizes that there are no acceptable human analogues of most of the techniques mentioned

above to study animals, with the exception of the DG technique. Functional mapping with FDG and other tracers will be the primary tools, at least for the foreseeable future, with which to study the organization of the human brain.

STUDIES OF THE RESTING AND PHYSIOLOGICALLY ACTIVATED HUMAN BRAIN

To investigate cerebral organization in humans, it is possible to study normal volunteers with FDG during a variety of sensory, motor, and cognitive stimulation tasks. In order to interpret the effects of such stimulation, and to evaluate the effects of various brain abnormalities, it is essential to have an appropriate group with which to compare the stimulation studies. The definition of this control group has not been trivial, since there is no resting state during which the brain is devoid of metabolic activity. Perhaps the most logical set of conditions would seem to be a resting state during which the subject receives no external sensory stimulation, performs no motor action, and is not asked to entertain any particular mental task, but this state of relative sensory deprivation has led to some surprising findings. Although in our studies we found no significant left-right asymmetries in subjects studied with both eyes and ears closed,²⁷ in a larger series, Mazziotta et al²⁸ found a consistent depression of metabolism in some right hemisphere structures under these conditions. Significant asymmetries of 3% to 7% were found in the visual association, posterior superior temporal, and inferior prefrontal regions, while such asymmetries were not present in the eyes open-ears closed or eyes closed-ears open states.

When subjects are studied with both eyes and ears open to low levels of ambient room light and sound, symmetrical uptake of FDG is seen throughout the brain²⁹ (Fig 1). Finklestein et al,³⁰ studying blood flow and oxygen metabolism, have reported left hemispheric activation in some, but not all, normal subjects. The possible reasons for these discrepancies are multiple and include (1) instrumentation differences, (2) variability in the details of test conditions, and (3) variations in individual neuropsychologic states. The appropriate control group for any given study will differ depending on the design of the study and the hypotheses to be tested.

There is less variability in the repeat measure-

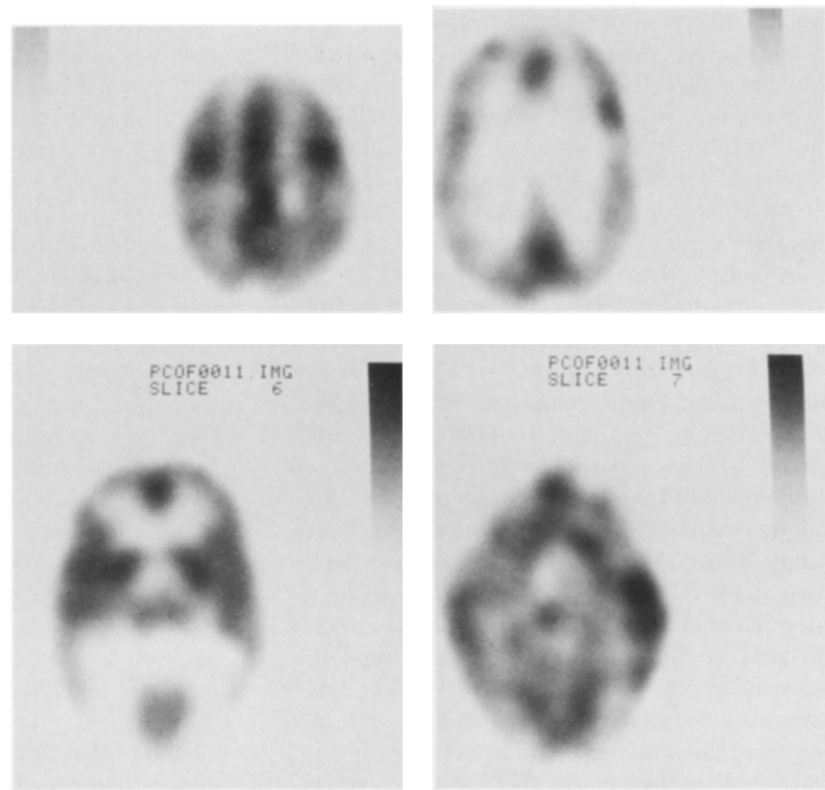


Fig 1. Normal study. Selected cross sections of the brain in a normal volunteer. Increased tracer concentration (black area) is noted in the gray matter of the cortex and internal gray matter structures. The white matter uptake of the tracer, compared with the gray matter, is less intense. These functional tomographic images correspond well to the comparable anatomic slices of the brain. (The subject's left is to the left of the observer in these images and in the other images in this report).

ment of metabolic rates within a single subject than in measurements across a group of subjects under identical conditions. In addition, one of the problems in functional imaging is the correct identification of the underlying anatomical structures. There is considerable variability from person to person in the size and location of a given structure,^{31,32} so comparisons between subjects have this additional complication. Evaluation of repeat studies in the same subject is facilitated by the knowledge that the underlying anatomy is identical. Using (^{C-11})DG, it is possible to perform repeat measurements on a subject within two to three hours because of the 20-minute half-life of C-11. The coefficient of variation of repeat measures in cortical areas ranged from 5.2% to 8.7% in subjects we studied twice under identical conditions with this compound.³³ Recently, some investigators^{34,35} have performed repeat studies on the same day with FDG, and Brooks et al³⁵ have reported reproducibility comparable to that obtained with (^{C-11})DG.

The first studies of the somatosensory system were performed on the positron emission transax-

ial tomograph III (PETT-III),³⁶ a device with relatively poor spatial resolution. We found that, in subjects in whom one hand was stroked lightly with a brush, the contralateral postcentral gyrus was 9% more active than the ipsilateral cortex. However, this result was not significant, probably because of partial volume effects and the difficulty in properly determining the anatomic site of the somatotopic representation of the hand area in all the control and stimulated subjects.^{27,37}

Using a higher resolution tomograph, the ECAT II,³⁸ Phelps and Mazziotta explored the normal response to a motor task consisting of unilateral finger movements. They found activation of approximately 19% in the contralateral precentral and supplementary motor cortices.³⁹

The auditory system has been studied extensively using FDG and PET technology. In mammals, the majority of projections from the cochlea are to the contralateral temporal lobe, while in humans we know that the left peri-Sylvian region is specialized for language functions^{40,41} (in the vast majority of right handers). The exact stimulus characteristics of the auditory task

appear to govern the cortical response. We have found that, in subjects listening monaurally to a meaningful English story, the contralateral superior temporal lobe is activated more than the ipsilateral cortex, with additional increases observed in the left inferior prefrontal area (Broca's area)²⁷ (Fig 2). When the task was modified to retain the linguistic characteristics but not the meaningful content (Hungarian story), the bilateral activation of the temporal lobe, contralateral greater than ipsilateral, was again observed, but no increase in metabolism was seen in Broca's area with the nonmeaningful stimulation.⁴² Mazziotta et al also found that stimulus content determined the distribution of glucose metabolism, but with slightly different results.⁴³ In a smaller series of subjects hearing a monaural English story, they observed a consistent activation of the left hemisphere regardless of the ear stimulated. They also examined auditory stimuli without language components and found that musical chords activated primarily right hemispheric structures (inferior frontal, parietal, and superior temporal). In subjects asked to discriminate between sequences of tones, their results depended on the scheme the subject used to make his determination. Musically sophisticated subjects, or those using analytic schemes, showed activation primarily of the left hemisphere, while musically naive or nonanalytic subjects were higher on the right side. Together, these studies demonstrate the well established specialization of the left hemisphere for verbal processing,

while suggesting that tonal and prosodic elements of language may activate right hemisphere structures. These results are consistent with clinical findings that show specific language deficits with specific cortical lesions. They also strongly support the view that multiple, widespread regions of the brain cooperate in the processing of complex sensory input.

In animals there are many regions of the brain that respond to visual stimuli,^{44,46} with some regions apparently specialized for processing highly specific features of the visual input. For example, Gross et al have found cells in the inferior temporal lobe of macaque monkeys that respond selectively to faces.⁴⁶ PET studies using FDG have been used to demonstrate the known afferent pathways to striate cortex, as well as to explore the response of peristriate and more remote areas to visual stimuli. It should come as no surprise that the specific details of the stimulus used determine the extent and magnitude of metabolic activation in visually responsive regions.

Phelps et al first demonstrated metabolic activation of striate (Brodmann's area 17) and peristriate (Brodmann's areas 18 and 19) cortex as a function of increasing stimulus complexity.⁴⁷ Both monocular and binocular stimulation resulted in symmetric glucose use in these areas, supporting the notion that in humans each eye sends half of its output to each side of the occipital lobe. Both regions progressively increased metabolism in response to stimulation

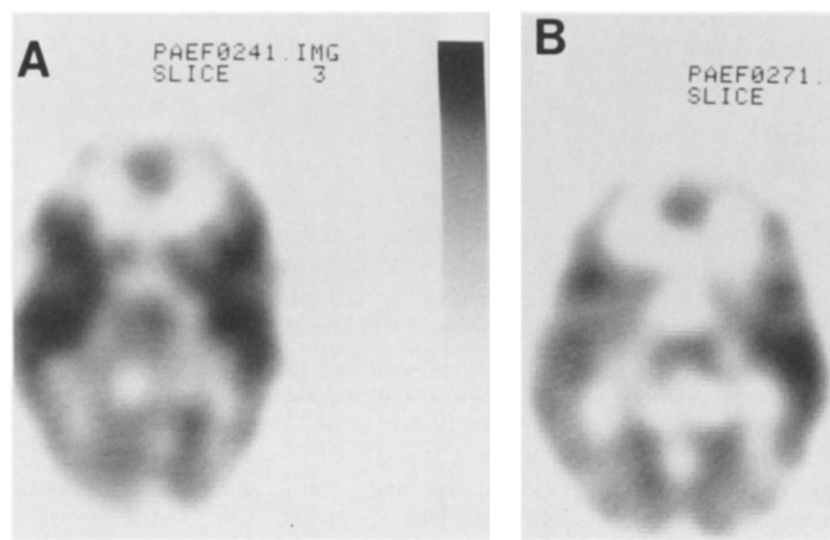


Fig 2. Auditory stimulation. (A) FDG image of a young, right-handed male volunteer who received auditory stimulation consisting of an English story presented monaurally to his right ear. Activation of the left superior temporal region is seen. (B) Image obtained in a second subject who listened to the story with his left ear. Metabolic activity in the right temporal region is greater than that in the left.

by white light, monocularly presented alternating checkerboard, binocular checkerboard, and complex outdoors scene, with the greater relative activation observed in the so called association areas. The metabolic increase with the complex scene, compared in the same subjects with the eyes closed control state, was 45% in the striate cortex and 59% above baseline in the peristriate regions.

Our PET studies of the visual system with FDG have been designed to demonstrate known pathways and to collect normative data with which to compare studies of patients with disruptions of the normal visual afferent system (Fig 3). Stimulation of one hemifield by a high-contrast black and white pattern of lines at various orientations resulted in significant acti-

vation (8%) of the contralateral striate cortex.^{27,37} We have recently extended these studies by varying the stimulus repetition rate and by presenting a checkerboard pattern to the central portion of one hemifield with simultaneous stimulation of the peripheral portion of the opposite hemifield. The central representation is known to project to the posterior portion of the calcarine cortex, while the peripheral representations project to anterior calcarine cortex. In order to present the stimuli to known portions of the visual field, the subject was required to fixate on a small light-emitting diode. Control subjects were studied who fixated on this diode without any patterned stimulation present. We also noted progressive increases in metabolism in the calcarine region among the various study groups.

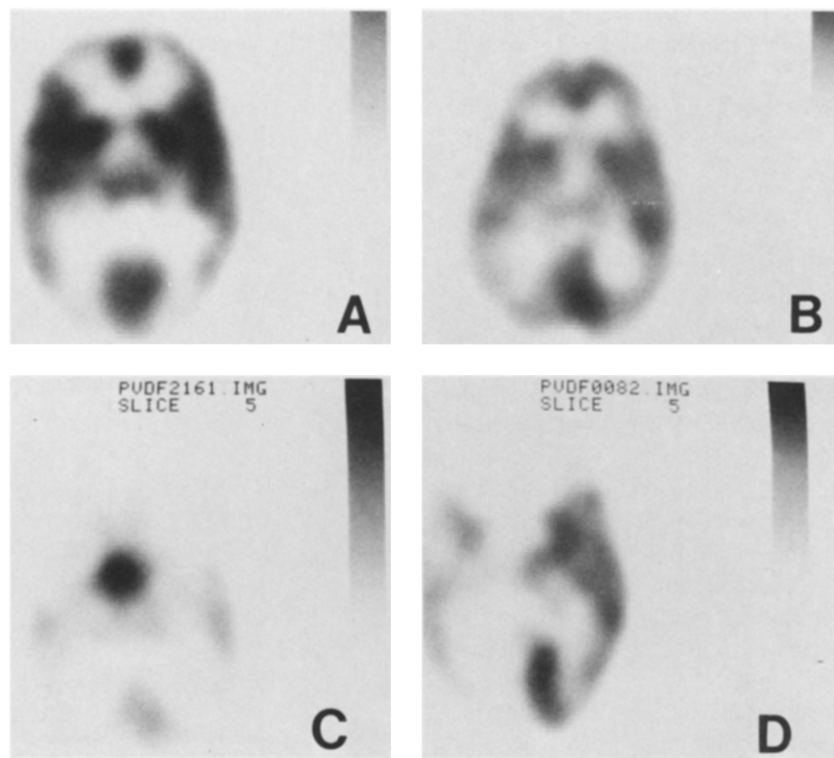


Fig 3. Visual stimulation. (A) Image of a normal volunteer studied with eyes and ears closed. Striate metabolic activity is symmetrical, but lower than other cortical regions under these conditions. Peristriate metabolism is very low in the absence of exogenous visual input. (B) Image of a normal volunteer whose left visual hemifield was presented with a flashing checkerboard pattern. Note activation of the striate cortex, with greater activity in the cortex contralateral to the field stimulated. Striate activity is greater than other cortical regions, while peristriate cortex is also activated when compared with (A). (C) A patient with a lesion of the optic chiasm caused by a pituitary adenoma. The left occipital cortex was completely deafferented by also patching the left eye, while the right eye received full-field stimulation. Note the decreased metabolism in the left striate region, as well as the hypermetabolic pituitary tumor. (D) Image of a patient with a complete right homonymous hemianopia due to occlusion of the left posterior cerebral artery. Glucose metabolism in the left striate cortex is almost totally absent, and depressed metabolism throughout the left hemisphere is apparent as well.

Eyes open controls were more active than eyes closed, while the diode control group demonstrated significant bilateral activation in the posterior calcarine cortex. Patterned visual stimulation produced the greatest metabolic response, with the most significant and most pronounced effect occurring in the posterior cortex contralateral to the central stimulus. Progressive activation in the peristriate regions paralleled the increases in calcarine metabolism. No consistent activation of the anterior calcarine cortex was seen to result from the peripheral stimulation, probably because of the low resolution of the PETT-V scanner.⁴⁸ We also found that the metabolic response of the calcarine cortex, but not of any other areas, depended on the frequency of pattern reversal. Compared with eyes closed controls, the posterior calcarine cortex was 9% more active, with a stimulus frequency of 5 Hz but 20% higher at 10 Hz. Similarly, the anterior calcarine cortex was 3% higher at 5 Hz and 11% higher at 10 Hz.⁴⁹ These findings agree with those of Fox and Raichle,⁵⁰ who used PET to study blood flow in volunteers receiving visual stimulation. They found that the maximum striate response occurred at a stimulus frequency of 8 to 16 Hz.

We also studied patients with lesions at different sites in the afferent pathway. Three patients with lesions of the optic chiasm causing temporal hemianopias were studied under the following conditions: Each patient received full-field monocular stimulation with a checkerboard pattern flashing at 10 Hz while fixating on a light-emitting diode. The contralateral eye was patched, resulting in complete pregeniculate deafferentation from visual input of the occipital lobe, which was anatomically and functionally normal. In each case, glucose metabolism in the striate cortex ipsilateral to the eye stimulated was significantly higher than the contralateral, deafferented cortex. One patient with bilateral hemianopias had a second study with binocular stimulation, which resulted in symmetric uptake in the striate cortex.⁵¹ Patients with ischemic damage limited to the optic radiations have been found to have reduced metabolism in the portion of striate cortex appropriate for their visual field defects. Patients with ischemic damage to the occipital lobe have more severely reduced glucose metabolism in regions that are also predictable

by their field defects.⁵² These and other studies^{47,53} have shown the ability of PET to map glucose metabolism within the visual system of the human brain.

A variety of approaches have been used to analyze PET images, each with its own merits and limitations. Areas that are functionally active may not correspond to clear anatomic boundaries, so some technique is required to relate the physiologic data obtained from the PET scan to the underlying anatomic structure in a reproducible manner, using commonly accepted terminology. Much of our data has been obtained using a computerized overlay system based on average anatomy⁵⁴ (Fig. 4). Regions of interest were defined from cadaver brains sectioned in the plane of PET imaging, and the average sizes and coordinates of each region were stored in a series of overlays that are scaled to match the corresponding FDG images. This is an objective way to define regions of

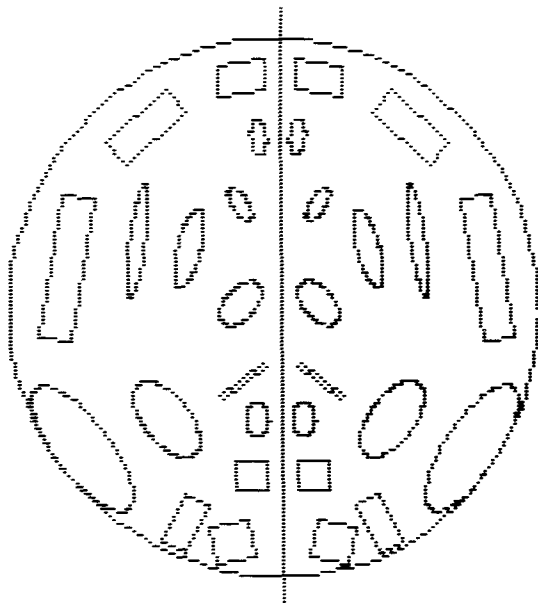


Fig 4. Computerized atlas overlay. Regions of interest based on average size and position of various structures are stored in a series of computer overlays. The overlay shown corresponds to a section at the basal ganglia level. The user selects the appropriate overlay and scales it to match the edge of the brain on the section image. As the overlay expands or contracts, the size and coordinates of each region expand or contract proportionately, with both x and y dimensions independent. The symmetrically placed regions of interest can be rapidly repositioned, reoriented, and changed in size to account for individual anatomic differences.

interest (ROI), and allows the very rapid analysis of hundreds of ROIs, but it may suffer with respect to accuracy. If an atlas-based approach is to be used, more than one atlas may be required depending on the age, handedness, and perhaps sex of the subjects. As with other stereotactic approaches,^{55,56} this technique makes assumptions about the relationship between external landmarks and brain structures in the images which may not be totally valid. We have extended the technique by matching the overlays with the appropriate magnetic resonance images (MRI) or x-ray computerized tomography (XCT) scans, which places multiple ROIs in their approximately correct positions. The ROIs can then be rapidly moved to the correct position based on the observed anatomy, and the adjusted overlay used to calculate metabolic data from the corresponding PET images.⁵⁷

Herholz et al⁵⁸ have developed another computer-based technique, which uses the PET image itself to determine regional boundaries. The computer program searches within raw regional contours to detect the edges of local metabolic activity. There is ample opportunity for the user to interact in order to make necessary corrections. This system has high reproducibility, largely independent of the user, while allowing for variations in individual anatomy. Inhomogeneities in pathologic tissue, however, may lead to inaccurate determination of boundaries, in which case the ROIs must be defined by the user or by assuming standard ROIs. We and others^{59,60} have also explored a technique that allows the computer to perform elastic matching of XCT, MRI, or PET images with a standard atlas. This approach can account for individual variability in size, shape, and angle of the brain within the cranium. To date no metabolic data have been reported using this approach.

Recognizing the complexity of the problems faced in attempting to analyze physiologic images of the brain, Mazziotta has recently initiated a series of workshops, under the sponsorship of the National Institute of Mental Health (NIMH), designed to develop a common set of standards, techniques, and terminology for all centers involved in functional brain imaging.⁶¹ We applaud these efforts, which should lead in the near future to standardized methods of analysis that can be applied to all types of studies, in

all subjects, with any available imaging system. While this is a worthwhile goal, it must be recognized, as Duara has recently pointed out,⁶² that all of the methods currently used have their limitations in practice as well as in theory. Patient motion can never be completely eliminated, and we must analyze the images actually obtained rather than the images we intended to obtain. We feel that no matter what positioning devices and analysis schemes are used, it is essential that an experienced observer interact with the computer in order to obtain the best possible estimates of regional glucose metabolism.

The complex organization of the brain suggests that metabolic changes in one region may affect metabolic measurements in both adjacent and distant regions. It seems likely that areas that are functionally associated will have significantly correlated metabolic rates. Metter et al⁶³ and Horwitz et al⁶⁴ have studied the intercorrelations of glucose metabolic rates among selected brain regions in normal adults, as a necessary step toward understanding how these normal relationships are disrupted in pathologic states. Metter et al first converted glucose metabolic rates to a "reference ratio" by normalizing regional values to the global metabolic rate, an approach used by many investigators to minimize the effect of differences in absolute metabolism. Both groups reported significant correlations between homologous regions in the two hemispheres, and strong correlations between frontal and parietal regions. Metter et al reported a negative relationship between frontal and posterior regions, and a reliable correlation involving the inferior frontal, Broca's, Wernicke's, and posterior temporal regions. Horwitz et al found correlations among temporal and occipital lobe areas and between primary somatosensory areas and premotor association areas. This technique should prove to be valuable in determining which regions of the brain act together under different conditions, as well as which regions do not, and provide a better understanding of both normal and abnormal functional pathways.

AGING AND DEMENTIA

In a group of eight infants, ranging in age from 5 days to 1 year, development of cerebral organi-

zation was determined using the FDG technique.⁶⁵ Infants from 5 to 26 days of age showed prominent metabolic activity in the sensorimotor cortex, thalamus, midbrain, brainstem, and cerebellum. Association cortices and the basal ganglia appeared relatively inactive. By 12 weeks, metabolic activity was noted in the basal ganglia and much of the temporoparietal association cortices. By 1 year, the pattern of glucose metabolism resembled that of normal adults, including prominent frontal activity. Older retarded children (2 years old) showed patterns similar to that seen in several day-old infants.

Kuhl et al determined LCMR_{glu} in 40 normal volunteers using the FDG technique.⁶⁶ At age 78 mean CMR_{glu} was, on the average, 26% less than at age 18. This alteration was of the same order as the variance among subjects at any age. Glucose consumption was symmetric in the hemispheres. The mean glucose metabolic rate in cortex, caudate, and thalamus was equal in each age group by decade. The slopes of decline of metabolic rates with advancing age were similar for cerebral cortex, centrum semiovale, caudate, and putamen. However, the metabolic rate ratio of superior frontal cortex to superior parietal cortex declined with aging. Several investigators report no age-related changes in glucose use.⁶⁷⁻⁷³

To determine regional cerebral metabolic changes with normal brain aging and dementia, we have studied 17 patients with probable Alzheimer's disease (AD) 11 elderly controls, and 11 young controls.⁷⁴⁻⁷⁶ All PET studies were done under similar resting, unstimulated conditions (eyes open, ears unplugged, dimmed lights, low level ambient machine noise). In patients with AD and control subjects, LCMR_{glu} was determined using an atlas overlay system.⁵⁷ Regional values were normalized to the mean whole brain values (Table 2). When young normal subjects were compared with elderly normals, we noted a significant relative decrease in frontal metabolism with aging, and a corresponding relative increase in posterior metabolism, especially in the calcarine cortex. In addition, the elderly normals demonstrated significantly reduced metabolism in the right inferior parietal region.

In patients with mild to moderate AD, there was a further decrease in inferior parietal metabolism beyond that noted with normal aging. Primary sensorimotor, visual, and cerebellar

Table 2. Significant Changes in Pattern of Regional Metabolism With Aging and Dementia (Numbers Represent Regional Metabolic Rate/Whole Brain Metabolic Rate × 100)

Region	Controls		AD	
	Young	Old	Mild-Moderate	Severe
L Frontal*	107	97†	95	75
R Frontal*	110	98‡	97	83
L Temporal*	92	95	89	79†
R Temporal*	96	101	92	89
L Inferior parietal	79	74	62	43‡
R Inferior parietal	83	79	67	56
L Sensorimotor*	104	98	105	111§
R Sensorimotor*	107	101	111§	117§
L Anterior calcarine	123	139†	139	179§
R Anterior calcarine	121	143§	145	181†
L Posterior calcarine	107	124‡	114	160†
R Posterior calcarine	105	125§	121	155
L Cerebellum	102	109	117	146†
R Cerebellum	102	111	127	155†

Note. For statistical analyses old controls are compared to young controls; AD patients (both severity groups) are compared to old controls.

*Combined region of interest.

† $P < .01$ (two-tailed T test).

‡ $P < .01$.

§ $P < .005$.

metabolic function were relatively preserved in the AD patients, fitting with the standard clinical impression that AD affects higher integrative cognitive functions with preservation until late in the disease of crude sensory and motor functions. Severe patients demonstrated significant reductions in left hemispheric cortical and specifically perisylvian metabolism, which may explain disturbances of language function seen late in the course of AD (Figs 5 and 6). These preliminary data show that significant alterations in regional cerebral glucose metabolism as determined by PET do occur in aging and dementia, and reveal the potential for PET not only to detect metabolic abnormalities that underly known clinical characteristics of disease states, but also to reveal areas that may be of value for more detailed future clinical, pathologic, pharmacologic, and neuropsychologic investigation.

Frackowiak et al used the $^{15}\text{O}_2$ steady-state technique to study cerebral blood flows (CBF) and cerebral O_2 metabolism in 22 dementia patients (AD) and multi-infarct dementia [MID] and 14 normal controls.⁷⁷ The results of this study indicated that compared with controls, the AD group had a diminished CBF and a

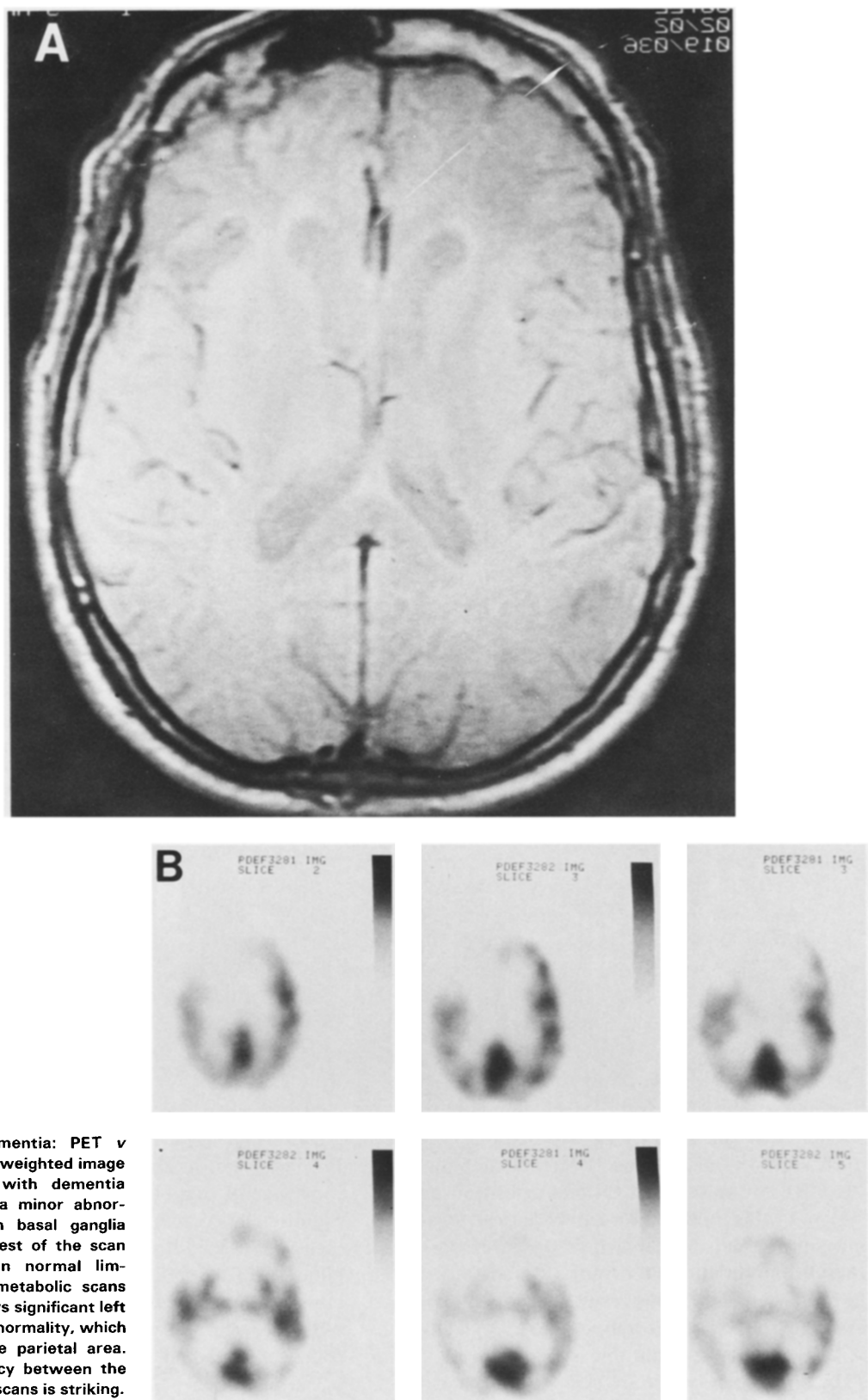


Fig 5. Dementia: PET v MRI. (A) A T2 weighted image of a patient with dementia demonstrates a minor abnormality in both basal ganglia regions. The rest of the scan appears within normal limits. (B) PET: metabolic scans with FDG shows significant left frontal lobe abnormality, which extends to the parietal area. The discrepancy between the PET and NMR scans is striking.

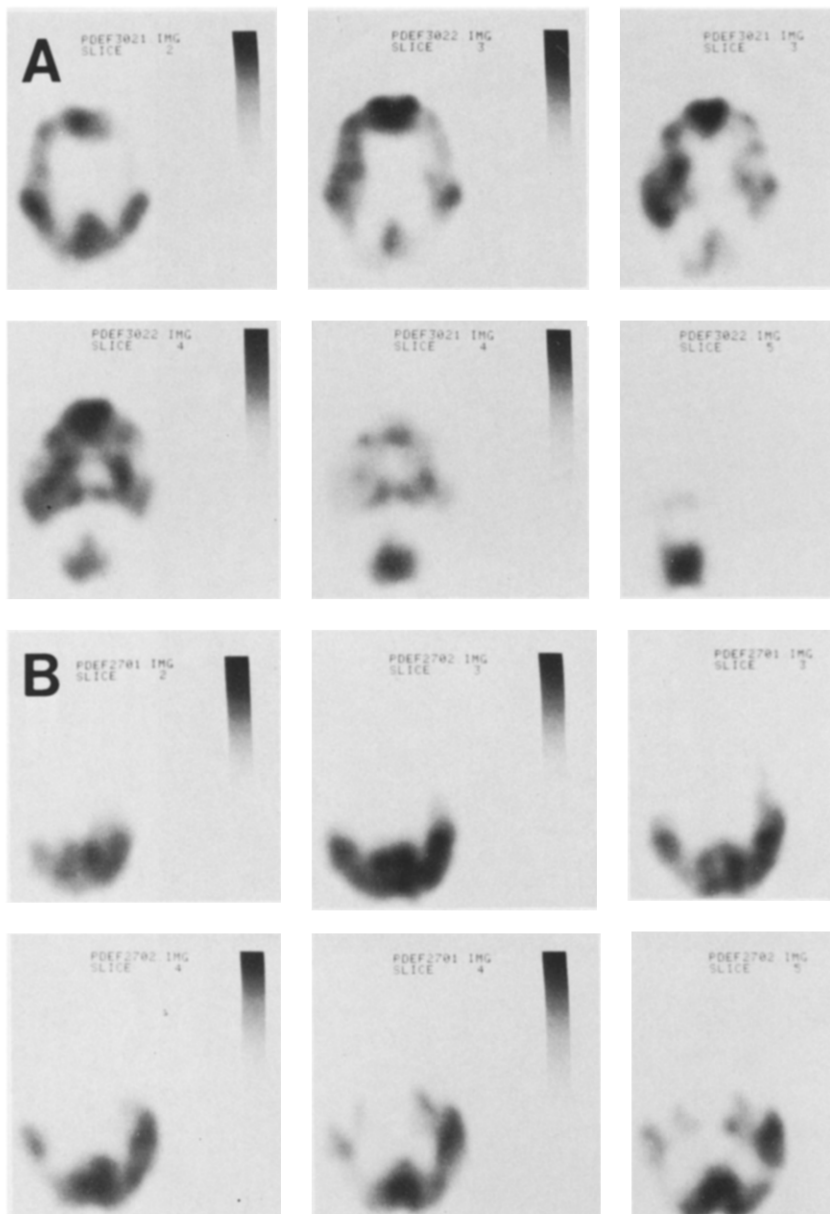


Fig 6. Patterns of metabolic abnormalities in dementia. (A) These images reveal predominant involvement of the temporoparietal lobes. This appears more impressive in the right hemisphere. Visual cortices, basal ganglia, and the anterior portions of the frontal lobes appear to be spared. (B) Metabolic images of a patient with advanced Alzheimer's disease show functional loss in the frontal, parietal, and temporal lobes. Posterior structures, especially the visual cortex, are well preserved. (continued on page 13.)

diminished metabolic rate for O_2 that was proportional to the severity of the disease. These authors also demonstrated a regional coupling of the CBF to the cerebral O_2 metabolism in both AD and MID. Furthermore, in both the degenerative and vascular groups, there was no change in the O_2 extraction ratio across different severity levels of dementia. This result supports the view that the brain changes found in AD or MID are not a consequence of chronic ischemia.

In another series of 24 AD patients and 22

elderly normal controls, significant decreases in glucose metabolic rates were found in AD.^{70,71} For regions of interest at the basal ganglia level the range of diminution was from 17% to 23%. Significant correlations were noted between measures of cognitive impairment and the metabolic rate. A series of discriminant function classification analyses were carried out to determine the accuracy with which individual subjects could be classified as AD patients or controls, based only on the regional glucose use values. For

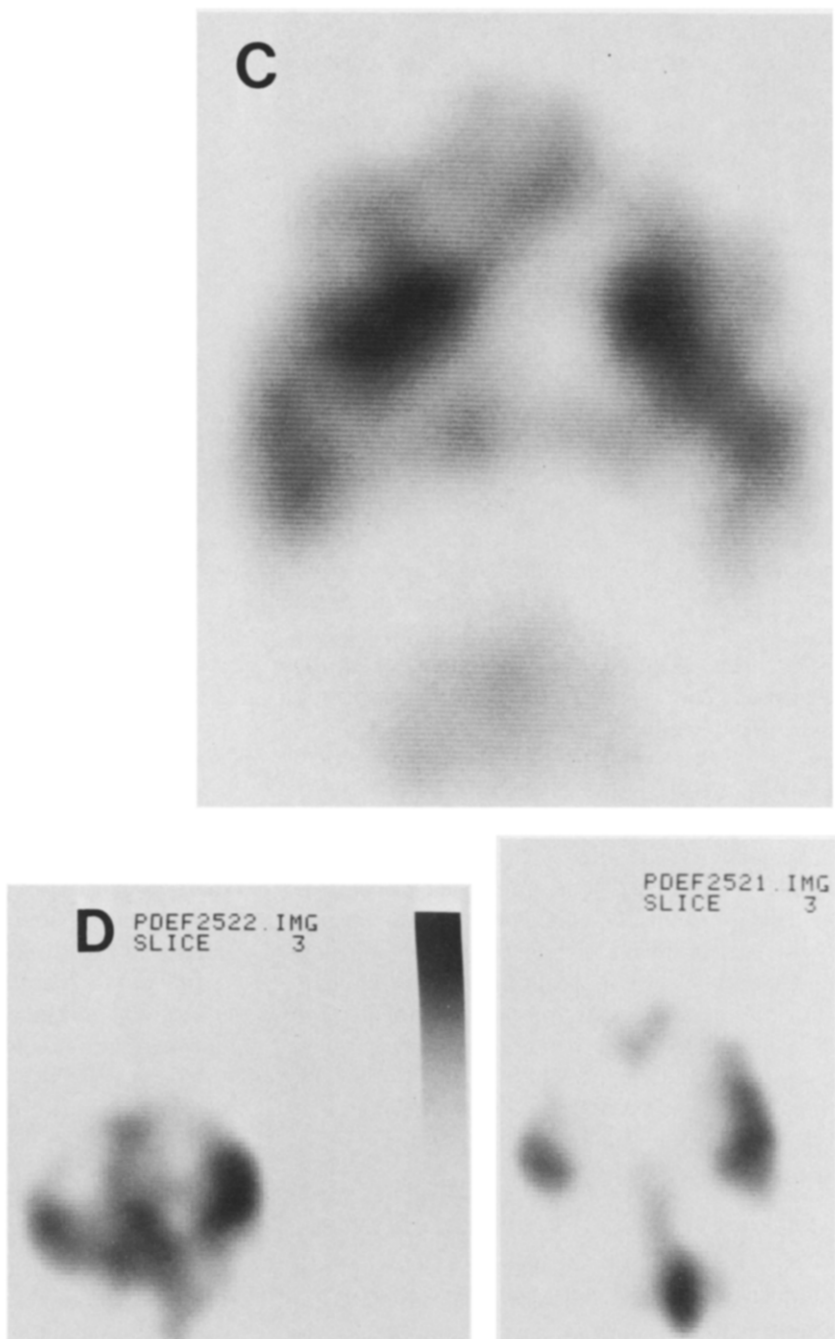


Fig 6. (cont'd) (C) All structures except for the basal ganglia are significantly affected in this patient. (D) These images demonstrate preserved metabolism in the somatosensory cortex as discussed in the text. This area is not affected early in the disease.

predictions based on single PET regions of interest, the overall classification accuracy ranged from 70% to 80%.

Foster et al studied 13 right-handed patients with AD using the FDG technique.⁷⁸ For this project, three subjects were selected with predominant language deficits, four with dispropor-

tionate failure of visuoconstructive function, and six who suffered primarily from memory loss. The group with language deficits showed marked reduction in LCMR_{glu} in the left frontal, temporal, and parietal regions. Those with predominant visuoconstructive dysfunction demonstrated focal hypometabolism in the right parietal cor-

tex. Patients with memory loss had no significant asymmetry of metabolic activity in cortical regions. The same investigators correlated psychometric testing with local cerebral metabolism in 17 patients with AD.⁷⁹ Compared with age-matched controls, global measures of intellectual function were 30% to 45% lower in the AD group. Similarly, mean cortical CMR_{glu} was reduced in the same group by 30%. There was a significant correlation between the degree of overall dementia and amount of metabolic decline. The most affected areas were the posterior parietal, posterior temporal, and anterior occipital regions. Frontal lobes were relatively spared. FDG PET data from Friedland et al were in general agreement with the above findings.⁸⁰

Since atrophy as demonstrated on current generation high resolution x-ray computerized tomographic (CT) scanners appears to be a feature of normal aging, dementia, and some other neuropsychiatric disorders, and given the relatively poor spatial resolution of currently used PET scanners, we have investigated the effect of CSF spaces on regional and global CMR_{glu} calculations as determined by PET.^{81,82} Since theoretically the CSF space has no metabolic activity, detailed quantitative measurements of this space (both in the cortex and the ventricles) should be carried out and taken into consideration in measuring regional blood flow and metabolism. Our preliminary data indicate that the metabolic rate may increase by 10% to 20% in elderly and demented subjects when corrected for atrophy. These early results also demonstrate that MRI may reflect the degree of cerebral atrophy more accurately than XCT scans (Fig 7).

PARKINSON'S AND HUNTINGTON'S DISEASE

Patterns of LCMR_{glu} have been determined in nine patients with Parkinson's disease (PD) as compared with normal control subjects.⁸³ No selective loss of metabolic activity was noted in the striatum where dopamine deficiency is the greatest. Compared with age-matched controls in patients with PD, LCMR_{glu} was moderately (18%) and uniformly reduced. With development of dementia and increased severity of bradykinesia, global CMR_{glu} decreased further. It is known that some parkinsonian patients with dementia demonstrate many pathologic and neurochemical features characteristic of AD. FDG-

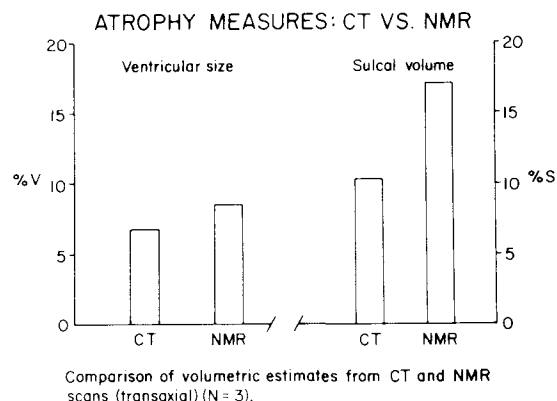


Fig 7. Atrophy detection: MRI v XCT. Comparison of volumetric estimates from MRI and XCT for ventricular and cortical atrophy are presented in this figure. Although ventricular volume as measured by both techniques is similar, XCT significantly underestimates cortical atrophy when compared with MRI.

PET studies of demented patients with PD have accordingly revealed significant decreases in the parietal cortex/caudate-thalamus ratio identical to that seen in patients with AD.⁸⁴ In patients with dementia (both PD and AD), this ratio correlated negatively with both the severity and the duration of the disease.

Huntington's disease (HD) is a genetic disorder that causes progressive dementia and chorea. This disease is characterized by widespread neuronal cell loss, particularly in the caudate, putamen, and cerebral cortex. In a study of this disorder, Kuhl et al examined 13 HD patients between the ages of 17 and 71, and 15 subjects 12 to 53 years old, who were "at risk" for the disease.⁸⁵ The head of the caudate is anatomically intact (by XCT) in the early HD subjects but becomes markedly atrophic in patients with advanced disease. In contrast, metabolic images reveal marked hypometabolism in the head of caudate compared to age-matched controls even in the early stages of the disease (Fig 8). The metabolic deficit appears to precede the gross structural changes that occur in this disease and this can be demonstrated by the disparity in the XCT and FDG scans findings. Global metabolic rate was not decreased in HD, in marked contrast to patients with AD who consistently show a generalized metabolic decline. In this study, approximately 50% of the at risk subjects exhibited caudate hypometabolism ($P < .001$) consistent with the autosomal dominant nature of HD. Of 15 at risk subjects followed at UCLA, three

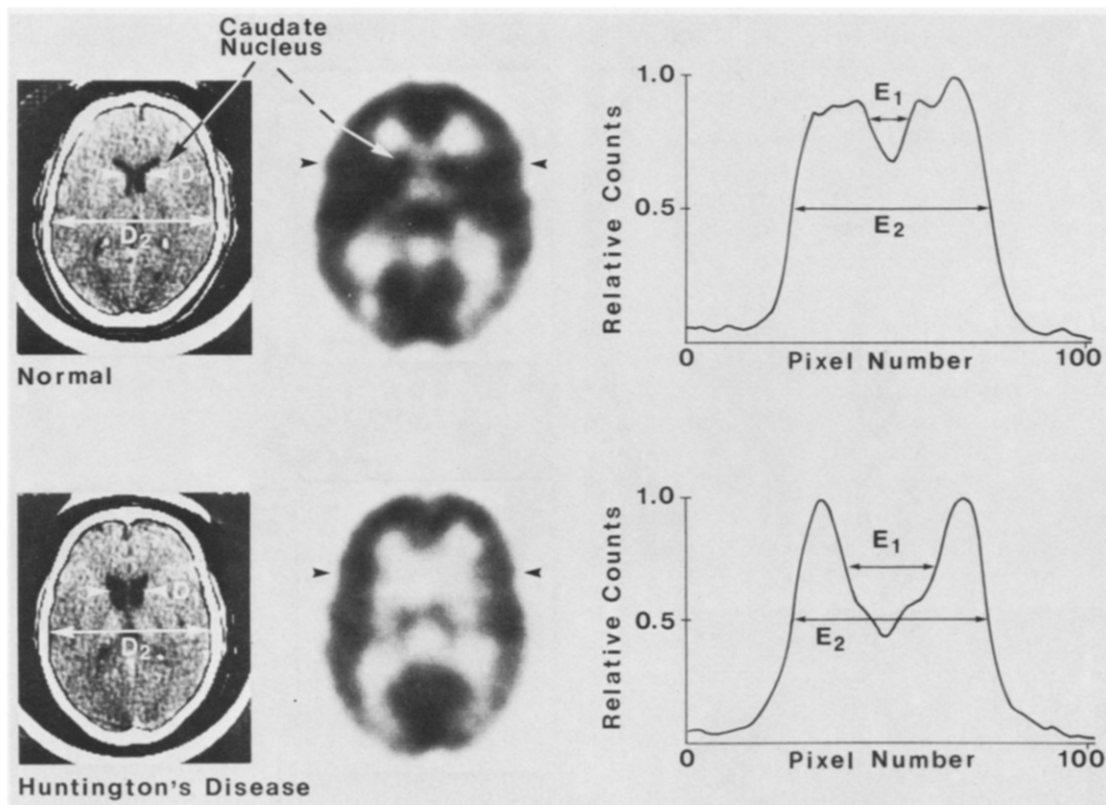


Fig 8. Huntington's disease. An FDG image of a patient with Huntington's disease reveals significantly diminished metabolic activity in the basal ganglia compared to a normal scan. Caudate XCT indexes and caudate metabolic rate (MR) indexes were measured as the intercaudate separations (D1 and E1) expressed as percentages of the bilateral diameter of the brain image (D2) or activity profile (E2). In the normal subject, the caudate XCT index was 10.8% and the caudate MR index was 18.0%. In a patient with Huntington's disease, the caudate XCT index was increased to 20.4% and the caudate MR index to 45.9%. (Reprinted with permission⁸⁵).

who had caudate hypometabolism when they were asymptomatic have gone on to symptomatic expression of the disease. This observation indicates that biochemical abnormalities in the at risk subject can be identified before the symptoms are apparent clinically.

A recent study using a higher resolution instrument has confirmed the above-described findings.⁸⁶ These authors also noted a significant correlation between disease duration and the ratio of caudate to putamen glucose metabolism. Their results indicate that metabolic alterations begin in the caudate nuclei and then spread to putamen as the disease progresses.

STROKE

The earliest reports of PET studies in stroke using $^{15}\text{O}_2$ and FDG indicated that PET could demonstrate abnormalities earlier than XCT, and with a wider topographic distribution.^{87,88}

Our own initial experience with 16 patients studied using FDG⁸⁹ 2 to 14 days after cerebral infarction revealed clear-cut lesions in 13 patients and probable lesions in two. Of the 15 patients with PET abnormalities, seven had unremarkable early XCT scans (Figs 9 and 10). The area of lowest metabolism corresponded to the area of radiolucency on XCT. However, the metabolic lesion tended to be larger than expected from XCT, especially with subcortical infarcts that exhibited hypometabolism of the overlying cortex. Four of the patients had additional XCT lesions suggestive of chronic infarction. These old lesions were well demarcated on PET and had no surrounding area of hypometabolism.

The phenomenon of "luxury perfusion", ie, LCBF in excess of local metabolic needs was noted in early PET ^{15}O investigations by Ackerman and Baron et al.^{87,90} During their first two

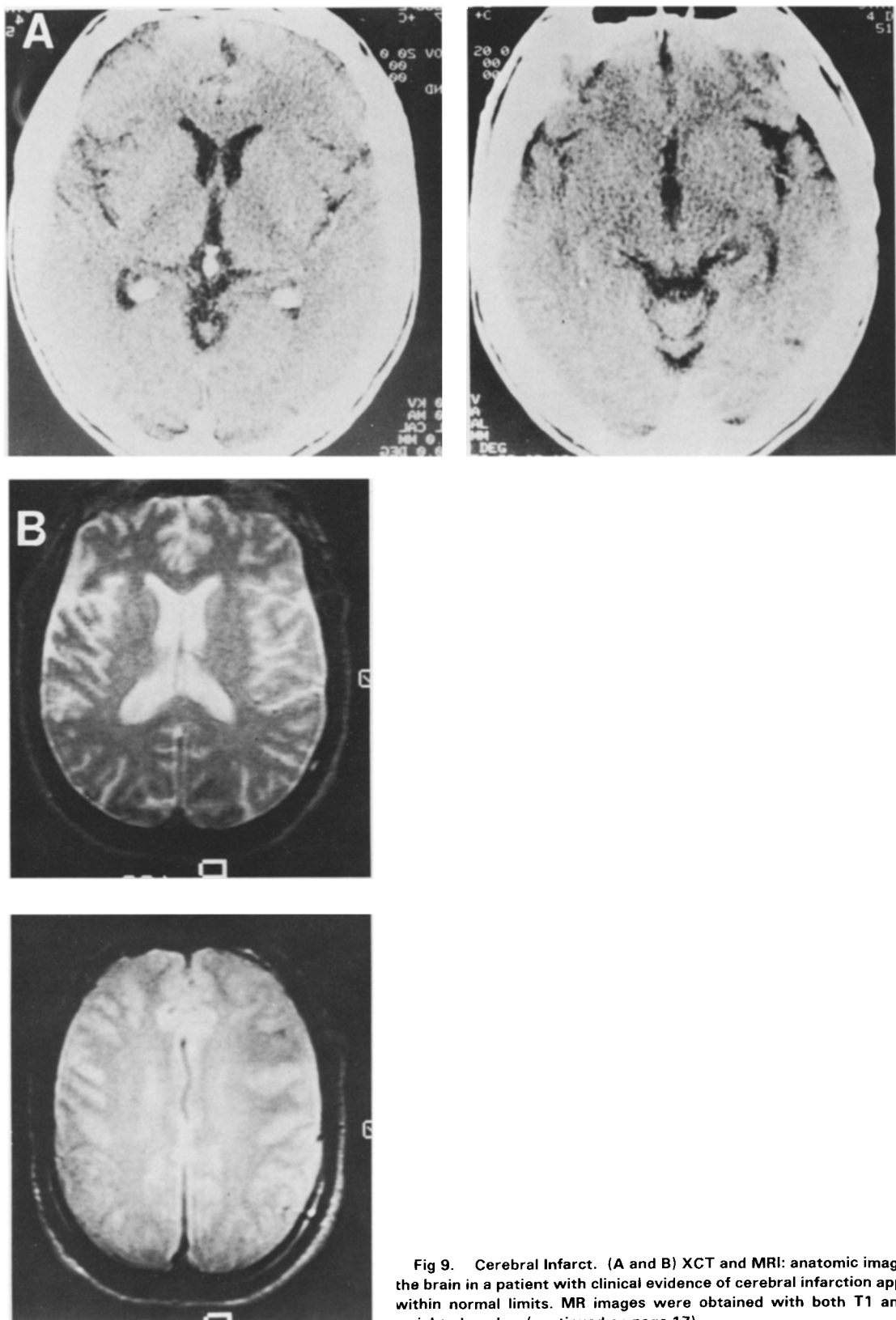


Fig 9. Cerebral Infarct. (A and B) XCT and MRI: anatomic images of the brain in a patient with clinical evidence of cerebral infarction appears within normal limits. MR images were obtained with both T1 and T2 weighted modes. (continued on page 17).

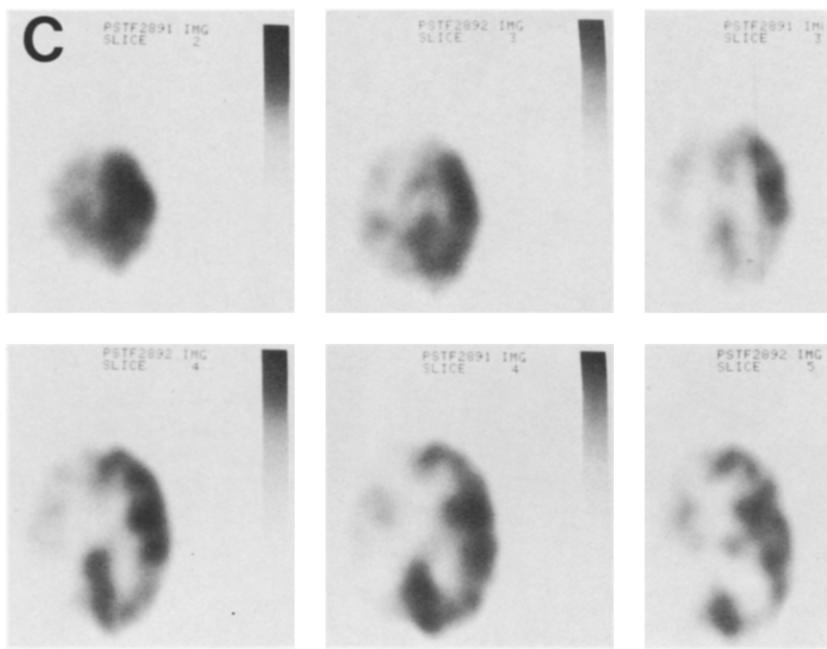


Fig 9. (cont'd) (C) PET metabolic images demonstrate extensive areas of reduced metabolism in the left hemisphere. A distinct region of abnormal metabolism is noted in the posterior temporoparietal area.

weeks postinfarction, some stroke patients demonstrated what Baron et al termed "misery perfusion," that is a relative increase in tissue oxygen metabolism compared to LCBF.⁹¹ Preliminary attempts to predict recovery from ischemia suggested that local cerebral oxygen metabolic rates ($LCMRO_2$) $< 1.25 \text{ mL O}_2/100 \text{ gm} \cdot \text{min}^{-1}$ foretell a poor clinical outcome, presumably secondary to completed infarction.⁹² LCBF is heterogeneous in these infarcted regions. Values below 10 to 20 $\text{mL}/100 \text{ gm} \cdot \text{min}^{-1}$ are generally associated with infarction.^{93,94} Low CBF may be appropriate to meet the negligible metabolic requirements of infarcted tissue. In this case, as under normal physiologic circumstances, CBF is coupled to metabolism.^{95,96} Baron et al found matched CBF-CMRO₂ in areas of infarction to be common after the tenth day postictus, indicating a normal oxygen extraction fraction (OEF).⁹³

Combined ^{15}O -FDG scanning sessions allow further description of altered oxidative metabolism in ischemia and infarction. As alluded to above, CMRglu is depressed in regions of infarction. When CMRO₂ and CMRglu are both measured within the core of infarcted tissue, the metabolic ratio of oxygen/glucose use is low.^{97,98} This is secondary to very low use of oxygen in the face of a better-preserved tissue ability to consume glucose. Cases have in fact been described

where the CMRglu is so well preserved, despite a low CMRO₂ and OEF, that the computed glucose extraction fraction (GEF) is above normal.^{97,98} Some uncertainty exists regarding the accuracy of PET CMRglu measurements in ischemic/infarcted tissue, given the lack of data on FDG rate and "lumped" constant changes under these pathologic conditions. Plausible pathophysiologic mechanisms can be postulated, however, to explain an elevated GEF in cerebral infarction.^{99,100}

Several recent PET investigations have sought to correlate various pathophysiologic aspects of early ischemia with the ultimate outcome of brain tissue at risk for infarction. Gibbs et al studied 32 patients with unilateral or bilateral carotid artery occlusions.¹⁰¹ These patients had presented with various neurologic problems including transient ischemic attacks (TIA), small completed strokes, and asymptomatic carotid occlusions. Ischemic symptoms ipsilateral to an occluded vessel occurred in 29 of 32 patients. Many of these patients had clinical features suggesting a hemodynamic basis for their symptoms. The ratio between local CBF and local cerebral blood volume (LCBF/LCBV) correlated well with local OEF. Values of LCBF/LCBV below 6.0 were associated with the highest OEF. All of these cases were classified as "hemodynamic ischemia" based on their clinical

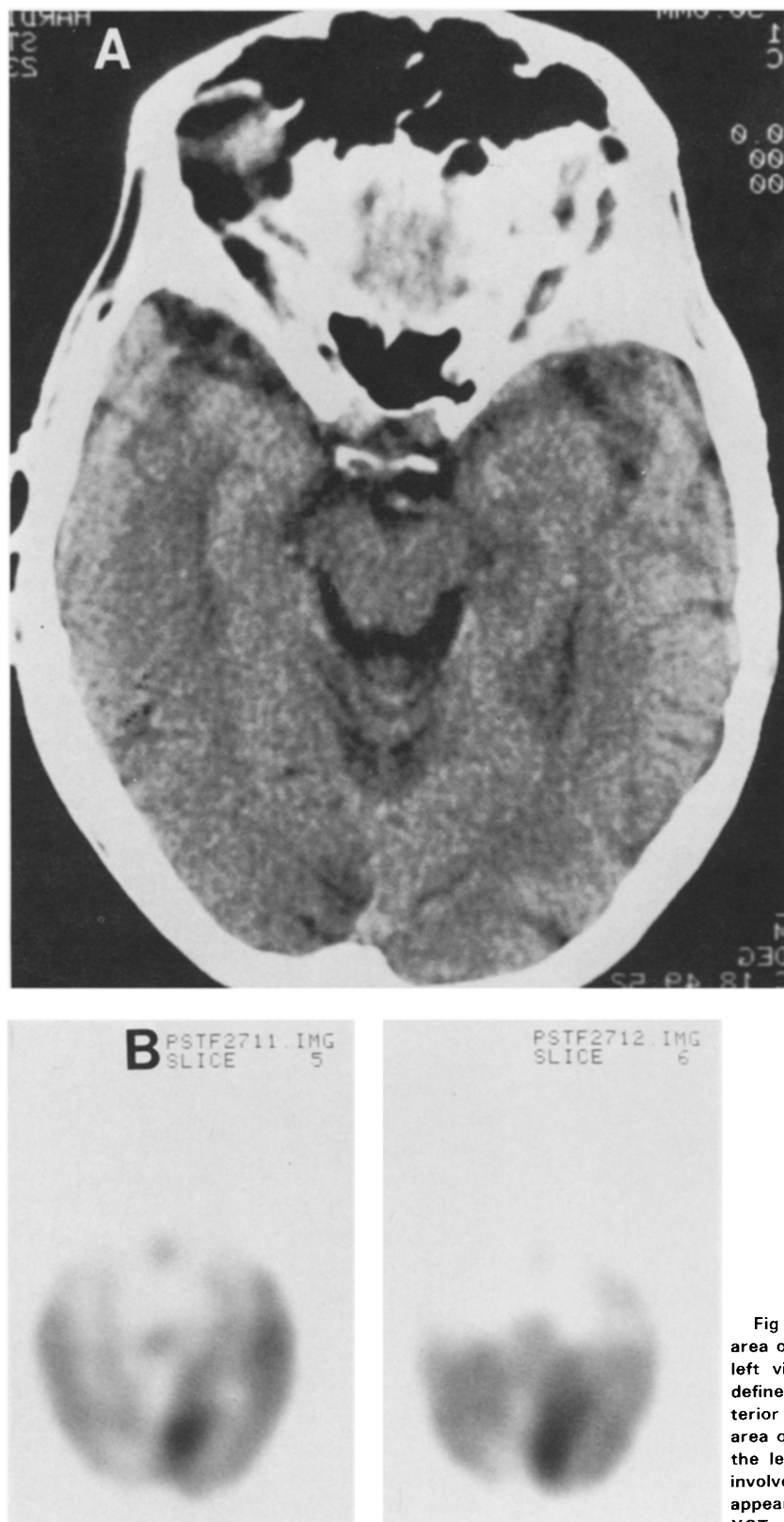


Fig 10. Acute infarct. (A) XCT: an area of decreased density is seen in the left visual cortex. This area is poorly defined and primarily confined to the posterior calcarine cortex. (B) PET: a large area of metabolic abnormality is seen in the left visual cortex. This abnormality involves the entire left visual cortex and appears much larger than that seen on XCT.

presentations. In most cases, low LCBF on the side of occlusion occurred in concert with a fall in LCMRO₂, even when there was no history of completed stroke and the XCT scan was normal. These results support the concept that ischemic changes may be present even when there are no symptoms of prolonged ischemia and the XCT scan is normal. As expected, the presence of a high LOEF occurs in the clinical setting of hemodynamic ischemia. The LCBF/LCBV ratio decreases progressively through the homeostatic stages of autoregulation and "misery perfusion" (increase in OEF) since CBV first increases while CBF is constant, then, when CBV is maximal, CBF declines. Therefore, this LCBF/LCBV ratio serves as a measure of "perfusion reserve" that can reliably quantitate the risk of future hemodynamic infarction.¹⁰¹ Powers et al have confirmed these results in a well-designed study. LCMRO₂, LCBF, LOEF, and LCBV were measured in a group of seven patients with histories of TIA and normal XCT scans.¹⁰² This group represents individuals at risk for further ischemia who have no clinical evidence of previous infarction. In regions with low CBF, CBV, mean transit time (CBV/CBF), and OEF, were all increased.

In addition to addressing diagnostic, prognostic, and therapeutic questions, PET investigations in stroke patients have provided intriguing and valuable insights into the functional organization of the brain. Kuhl et al in an early PET publication described two patients with decreased metabolism in an otherwise intact left visual cortex due to infarcts confined to the middle cerebral artery territory.⁸⁸ Both patients had right homonymous visual field defects. The left occipital cortex was clearly hypometabolic on the FDG PET scan, despite no loss of attenuation on XCT. Such hemodynamic or metabolic effects remote from the site of infarction termed "diaschisis" may explain stroke symptoms and signs for which no previous pathologic or morphologic correlates had been found. Kuhl et al reported hypofunctional zones in cerebral cortex, striatum, and thalamus ipsilateral to but remote from infarcted brain regions; all of these structures appeared normal on XCT scans.⁸⁸ Cerebral defects of metabolism and flow contralateral to areas of infarction, so called "mirror foci," were

observed by Lenzi et al and felt to represent interruption of transhemispheric connections.⁹² "Crossed cerebellar diaschisis" was first reported on PET images by Baron et al, who felt this to be an acute transient phenomenon.¹⁰³ Our own investigations also suggest that cerebellar hypometabolism contralateral to cerebral infarction is most prominent early in the clinical course.¹⁰⁴ The fact that flow and metabolism remain coupled (even if reduced) in these areas remote from the primary infarction suggests that the fall in CBF is secondary to metabolic changes occurring in a region of functional differentiation.^{98,105,106}

EPILEPSY

During focal or generalized epileptic seizures, both brain metabolism and blood flow are significantly elevated while both are depressed in the postictal and interictal states.^{107,108} In partial, as contrasted with generalized seizures, ictal activity and EEG manifestation of seizure activity are initially restricted to one region of the brain, while generalized seizures involve both cerebral hemispheres from the onset of the ictal event. Partial and partial complex seizures are often refractory to medical control, but may be treated surgically if the ictal focus can be accurately localized. While EEGs provide invaluable information about seizure activity, epileptiform findings in an EEG lead (even from a depth electrode) may reflect activity propagated from another site and may not accurately pinpoint the origin of the event.¹⁰⁹ Thus, flow and metabolic information obtained from PET studies is complementary to clinical and EEG data. XCT and MR scans are usually normal in patients with seizure disorders.^{81,110} Approximately 70% of patients with partial seizures have demonstrated one or more regions of hypometabolism on interictal FDG scans¹¹¹ (Fig 11). The location of the zone of hypometabolism correlates well with the site of the EEG focus determined from interictal and ictal scalp and depth electrode findings^{111,112} and with the site of histopathologic abnormalities noted on microscopic examination of resected specimens.¹¹³ However, the area of hypometabolism is consistently much larger than the area of structural damage.¹¹³ In most of the brain tissue that has been examined, pathologic lesions have

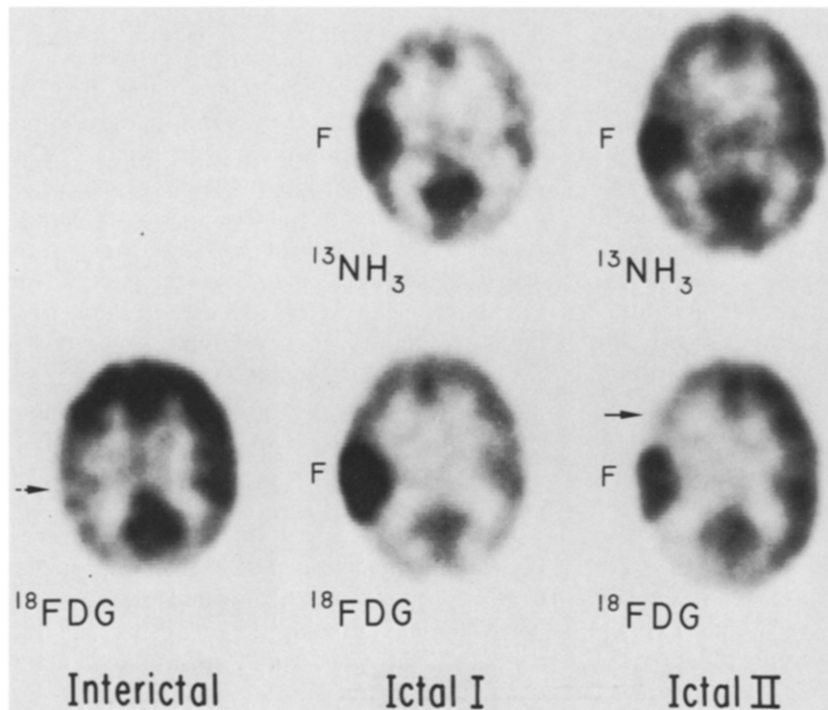


Fig 11. Seizure disorders. Interictal and ictal scans of a 5-year-old boy who had a 10-month history of right focal motor seizures. XCT, arteriography, and pneumoencephalography were normal. The interictal FDG scan shows hypometabolism in the left temporo-parietal cortex (dotted arrow). At the same site, ictal study twice shows marked focal hypermetabolism and hyperperfusion ($^{13}\text{NH}_3$ scans), coincidental with right facial twitching and epileptiform EEG spike activity in the left fronto-temporal region. (Reprinted with permission.¹¹⁵)

been limited to mesial temporal structures while the entire temporal lobe, lateral as well as mesial, is hypometabolic. When the histopathologic lesion is mesial temporal sclerosis, there is a good correlation between the amount of cell loss and the degree of decrease in LCMR_{glu} calculated for the hypometabolic zone.¹¹³ On the other hand, there is no correlation between the degree of decrease in LCMR_{glu} and either the frequency of interictal EEG spike discharges or the appearance of abnormal EEG slow wave activity.¹¹¹ The good correlation between the location of the zone of hypometabolism and the location of microscopically determined structural damage has made PET extremely useful in the verification of EEG-localized epileptogenic lesions for resective surgical therapy.^{109,112,114}

Ictal FDG studies have also been carried out on a number of patients during spontaneous partial seizures.^{112,115,116} The patterns of glucose use seen during ictal studies have been unique to each patient. Most patients show one or more focal areas of relative hypermetabolism that appear to represent the site(s) of seizure generation, as well as sites of ictal propagation. As with the interictal studies, there is no clear correlation

between the frequency or duration of ictal EEG discharges and the absolute or relative changes in metabolic activity during seizures.¹¹⁶

In patients with petit mal epilepsy, FDG scans have been carried out during hyperventilation, which produced frequent absences before medical treatment.^{117,118} These ictal scans exhibited diffuse increases in LCMR_{glu} compared with scans performed during hyperventilation following medical treatment, when no absences occurred. No areas of abnormal focal hyper- or hypometabolism were noted on ictal scans. In the interictal state, no metabolic abnormalities have been identified in these patients. In another study, interictal scintigrams in eight patients with primary generalized seizures did not show any focal hypometabolic areas.¹¹⁹

Patients with generalized seizures and the Lennox-Gastaut syndrome have been studied in our laboratory.¹²⁰ Some are candidates for corpus callosum section. These studies provide an opportunity to determine whether specific foci of hypometabolism can be consistently demonstrated in subtypes of this disorder, whether preoperative metabolic patterns can predict surgical outcome, and whether postoperative

improvement in seizures results in the resolution of these abnormal metabolic patterns. The latter is of particular interest in this patient population since the epileptogenic lesion or lesions are not surgically removed.

BRAIN TUMOR STUDIES

DiChiro et al pioneered the use of the FDG technique for the evaluation of brain tumors with PET.¹²¹ They have reported on a total of 72 patients.¹²² Most of their patients had biopsy-proven primary malignant brain tumors. Other patients had low-grade tumors by XCT criteria, but were never biopsied.

These investigators found a mean CMR_{glu} for low-grade tumors of 4.0 ± 1.8 mg/100 gm/min, which was similar to their values for normal white matter.¹²¹ For the high-grade tumors, they found a mean CMR_{glu} of 7.4 ± 3.5 mg/100 gm/min, similar to normal gray matter. In most of the high-grade tumors they found a hot spot by visual inspection of the scan, although this was an extremely rare finding in the low-grade tumors. In a group of 36 patients with high-grade gliomas, PET scans showed an increased metabolic rate of 28 patients and a decreased metabolic rate in eight patients. Of 33 patients with low-grade gliomas, PET scans showed an increased metabolic rate in four patients and decreased rate in 29 patients. In the majority of patients, localized metabolic suppression was seen in cortical areas adjacent to the tumor, or in areas neuronally connected to the tumor.^{123,124}

The findings on PET scans did not always correlate with XCT results. Hypermetabolic lesions always showed enhancement on XCT scans, but low activity PET lesions also showed enhancement about 50% of the time. In most cases where PET and XCT did not correlate, the PET was more accurate in predicting the degree of malignancy of the tumor. The PET technique was also used to study two cases of biopsy-proven radiation necrosis.¹²⁵ Although XCT cannot usually differentiate between radiation necrosis and recurrent tumor (since both appear as enhancing lesions), PET scans show a striking difference between these two disorders. Patients with radiation necrosis had hypometabolic lesions, whereas high-grade gliomas were always hypermetabolic. Thus, PET has been recom-

mended as the best available noninvasive technique to diagnose possible radiation necrosis.

In our center we have examined 24 patients with a history of brain tumor using the FDG technique.¹²⁶ Most patients had a biopsy diagnosis of malignant glioma. In general, patients with high-grade tumors were found to have hypermetabolic lesions while lower-grade tumors were hypometabolic (Figs 12, 13, and 14). On five PET studies, lesions appeared to have normal metabolism compared with healthy brain tissue. These lesions were all located in the white matter. Three were low-grade tumors (Fig 15), one represented radiation necrosis, and one was a grade IV glioma whose scan had been hypermetabolic before radiation therapy.

There was a good correlation between enhancement on XCT scan and the metabolic rate measured by PET. Of the lesions that enhanced intensely on XCT scan, 13 were hypermetabolic, and five were not. One of the hypometabolic lesions represented biopsy-proven radiation necrosis (Fig 16). This finding supports the results of DiChiro et al discussed above. The presence of a hypermetabolic lesion in one hemisphere was often associated with contralateral cerebellar hypometabolism.¹⁰⁴

We also found a correlation between metabolic rate and prognosis. Of the glioma patients whose tumors were hypermetabolic at any time in their course, 80% died during the follow-up period. The median survival of all of these patients from the time of diagnosis was 11 months. On the other hand, 25% of the patients with normal or low metabolic activity have died, and the median survival from diagnosis was 33 months, with a range of 1 to 7+ years. These findings correspond to those of Patronas et al.¹²⁷

PSYCHIATRIC DISORDERS

Buchsbaum et al studied eight unmedicated schizophrenic patients and six control patients using FDG.¹²⁸ They examined three transverse brain slices and reported relative hypofrontality at the supraventricular level in their psychotic patients. These investigators also reported increased activity in the left temporal lobe of schizophrenics, with lower left basal ganglia metabolism.

Farkas et al studied 15 schizophrenic patients

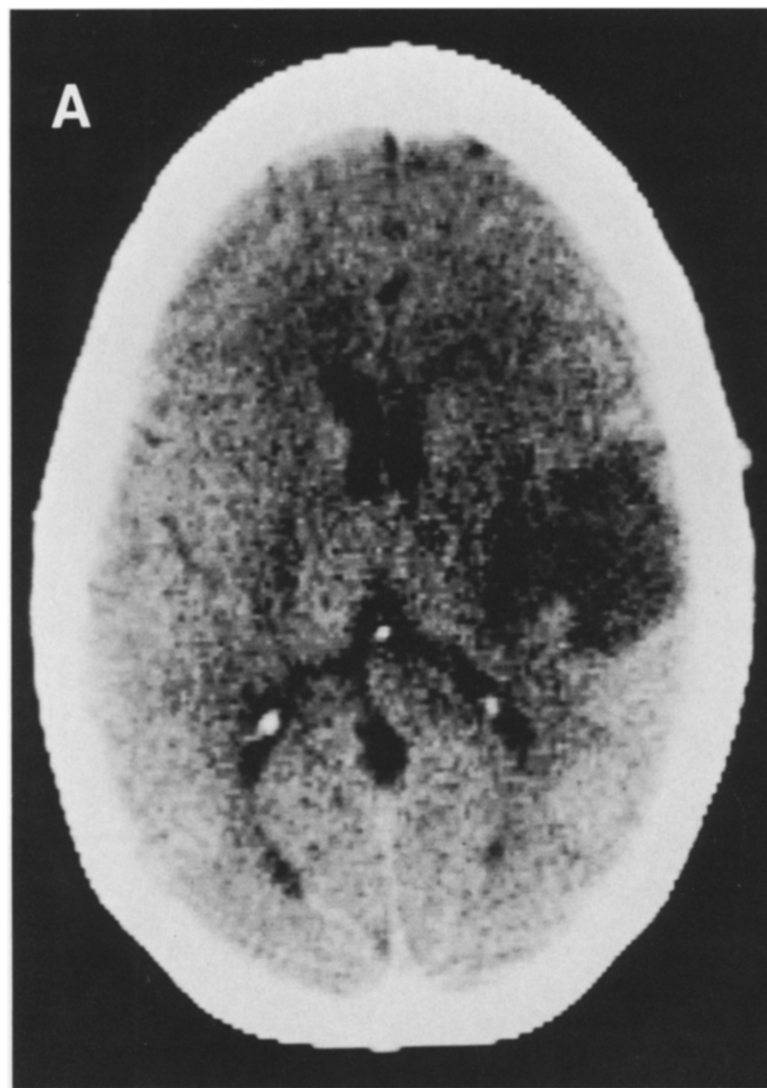


Fig 12. Low-grade glioma. (A) XCT: in this patient with a low-grade tumor detected five years earlier, an area of low density is seen in the right temporoparietal lobe. This lesion did not enhance following the administration of the iodinated contrast medium. (Continued on page 23.)

(seven unmedicated) and 11 normal patients using FDG.¹²⁹ Two PET slices were analyzed. Schizophrenics had relatively lower metabolic rates in frontal compared with posterior regions. There were no differences between medicated and unmedicated patients. Wolkin et al used FDG to study ten schizophrenic patients before and after "somatic treatment."¹³⁰ These patients were compared to eight normal controls scanned only once. Lower absolute metabolic rates in schizophrenic patients were observed in frontal and temporal regions before treatment. This hypofrontality persisted following treatment.

Using $^{15}\text{O}_2$ to measure LCBF and LCMRO₂, Sheppard et al scanned 12 schizophrenic patients

and 12 controls.¹³¹ Results from two PET levels were analyzed for ten patients using four different analysis methods. No evidence for hypofrontality was found with any method. One analysis revealed significantly decreased activity in basal ganglia of schizophrenics. Two data reduction techniques demonstrated a laterality effect, with schizophrenics showing higher left hemispheric flows.

Qualitative analysis of PET scan images (FDG) performed in our center indicates that scans of schizophrenic and control subjects can be reliably discriminated. Ten PET scans of schizophrenics and four scans of controls were randomly ordered and read as "normal" or "ab-

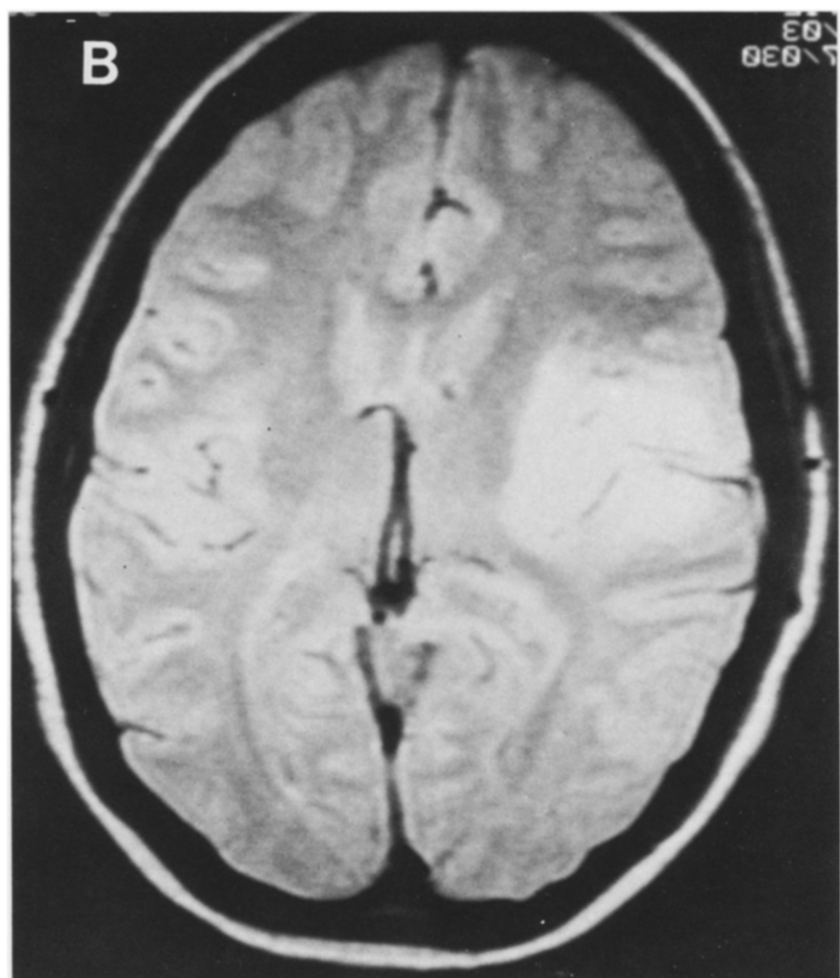


Fig 12. (cont'd) (B) MRI: a T2 weighted image of the brain shows an area of abnormal density in the right temporal lobe. This lesion corresponds exactly to the lesion seen on the XCT scan. (C) PET: corresponding to the site of the tumor, as seen on the XCT and MR scans, an area of decreased metabolic activity is seen on the PET study. The temporal lobe cortex adjacent to the tumor also appears hypometabolic.

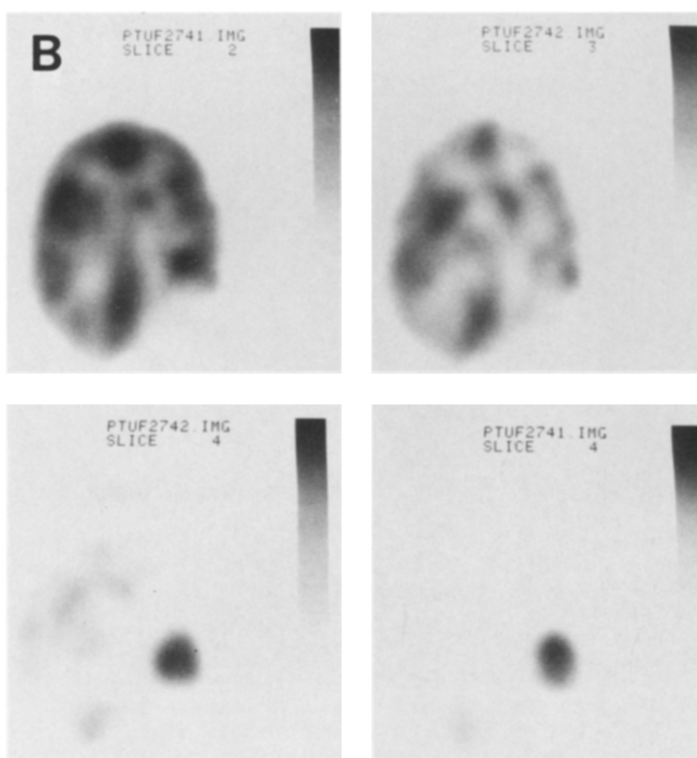


Fig 13. High-grade glioma. (A) XCT: a contrast-enhanced lesion is seen in the right temporoparietal area with cystic changes anterior to the abnormality. Some edema also is noted adjacent to the tumor. These findings are consistent with a high-grade tumor. (B) Metabolic scans with FDG shown in several planes reveal intense uptake in the contrast-enhanced lesion seen on the XCT images. The intensity of metabolic activity in the tumor is well demonstrated in the lower section slices. Functional activity of the anatomically intact brain adjacent and distant to the tumor is significantly decreased. In our experience this is a typical appearance for grade III and IV brain tumors.

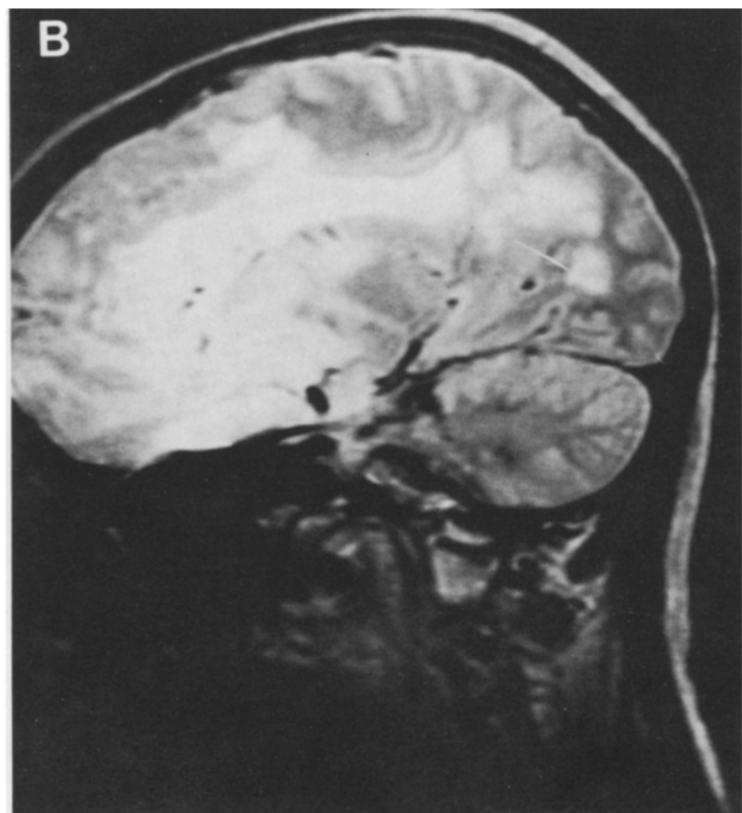
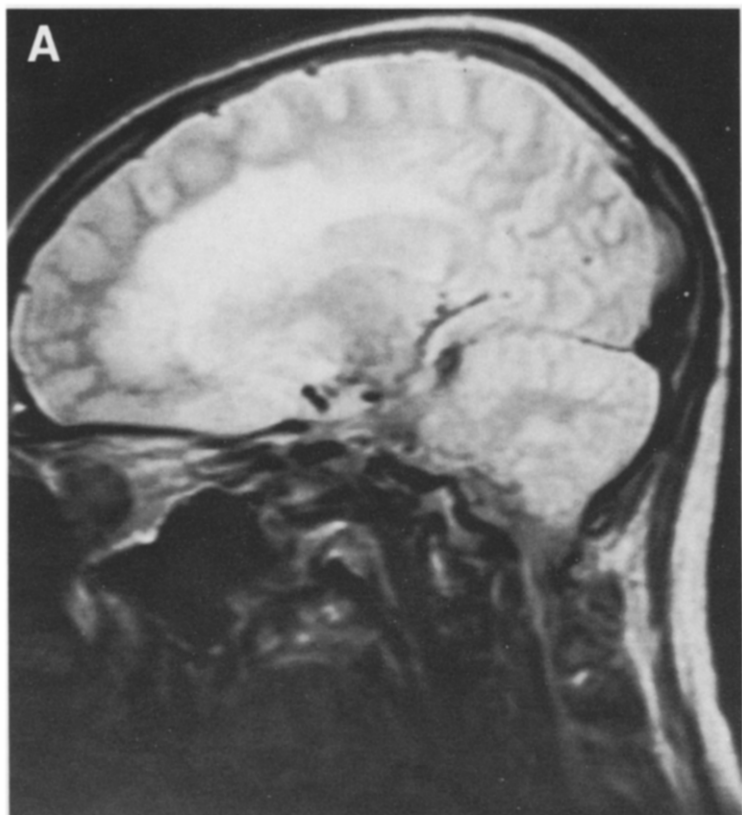


Fig 14. High-grade glioma. (A and B) MRI: two T2 weighted sagittal sections of the brain obtained on a patient with high-grade glioma are shown above. These images show the tumor distinctly in the left frontal lobe close to the midline. The grade of the tumor cannot be determined from these images. However, the most striking finding is the extent of the edema surrounding the tumor. The latter extended to the occipital lobe. The degree of edema on the XCT scans was less impressive. (continued on page 26.)

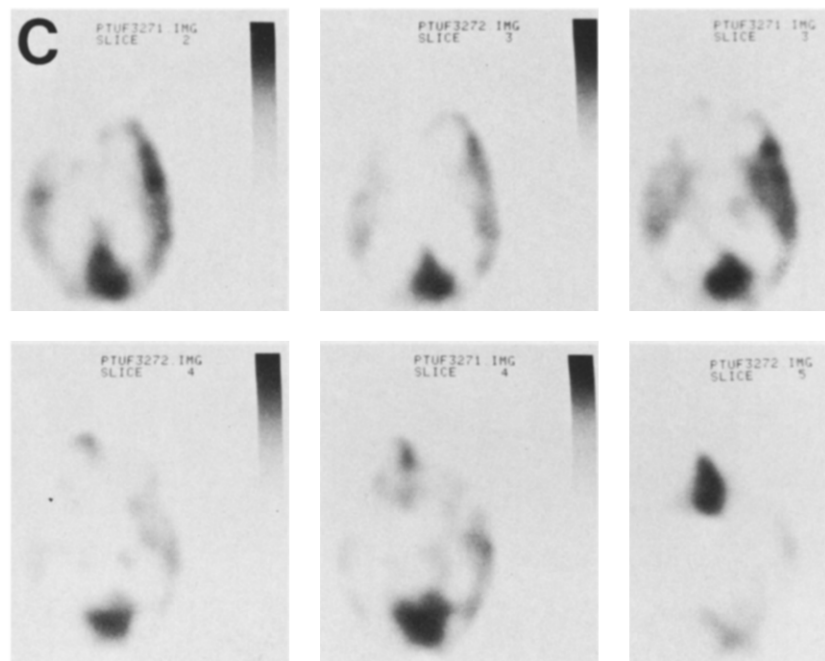


Fig 14. (cont'd.) (C) PET: transaxial images of the brain with FDG show an area of intense uptake in the left inferior frontal lobe, especially in a region adjacent to the midline (lower three images). Of interest is the presence of extensive metabolic decline in the left hemisphere. This probably is caused by the peritumoral edema seen clearly on the MR images.

“normal” by three investigators blind to subject diagnosis. Nine of the ten scans of schizophrenic subjects were read as abnormal, whereas all four scans of normal controls were read as normal. Thus, 13 of 14 (93%) of the scans were correctly classified. Metabolic images of most patients with schizophrenia revealed reduced metabolism in the left hemisphere, especially in the temporal lobe. Preliminary analysis of treatment effects has not demonstrated significant changes in metabolism between pre- and posttreatment studies.

During the depressive phase of bipolar psychosis, reductions of about 25% in glucose use throughout the supratentorial structures have been noted when patients are compared with the appropriate controls.¹³² In the hypomanic phase, the same patients exhibited metabolic rates that were not different from control values. Reduced glucose metabolism in these patients is global and diffuse throughout the brain, although some preferential changes are noted in the frontal and anterior cingulate cortices. In patients with unipolar mood disorder (depression) who were medication free, global metabolic rates were within normal limits. The latter group, however, did exhibit a significant decline of glucose use in the

corpus striatum that reverted to normal when the patients became euthymic.

PET, MRI, AND XCT CORRELATION IN CNS DISORDERS

In the past two and a half years we have studied 45 patients with a variety of neurologic disorders using all three tomographic modalities. These include primary brain tumors, dementia, acute and old infarcts, seizures, head injury, and psychiatric disorders.^{81,133}

In patients with primary brain tumors the XCT scan outlined the tumor size and location accurately in each case. MRI, obtained with a 0.12 Tesla unit, although it detected an abnormality in every case, did not appear to be significantly superior to XCT scan in most cases. The tumor margins were more accurately determined by the enhanced XCT scan. However, the extent of peritumoral edema was more clearly seen with MRI. Edema was better appreciated with T2-weighted images using a super-conducting magnet (1.5 Tesla, Signa) (Figs 14 and 15). On XCT, grade 3 and 4 tumors showed significant enhancement after contrast infusion (Figs 12, 14 and 16). MRI was unable to distinguish low-grade tumors from high-grade malignancies.

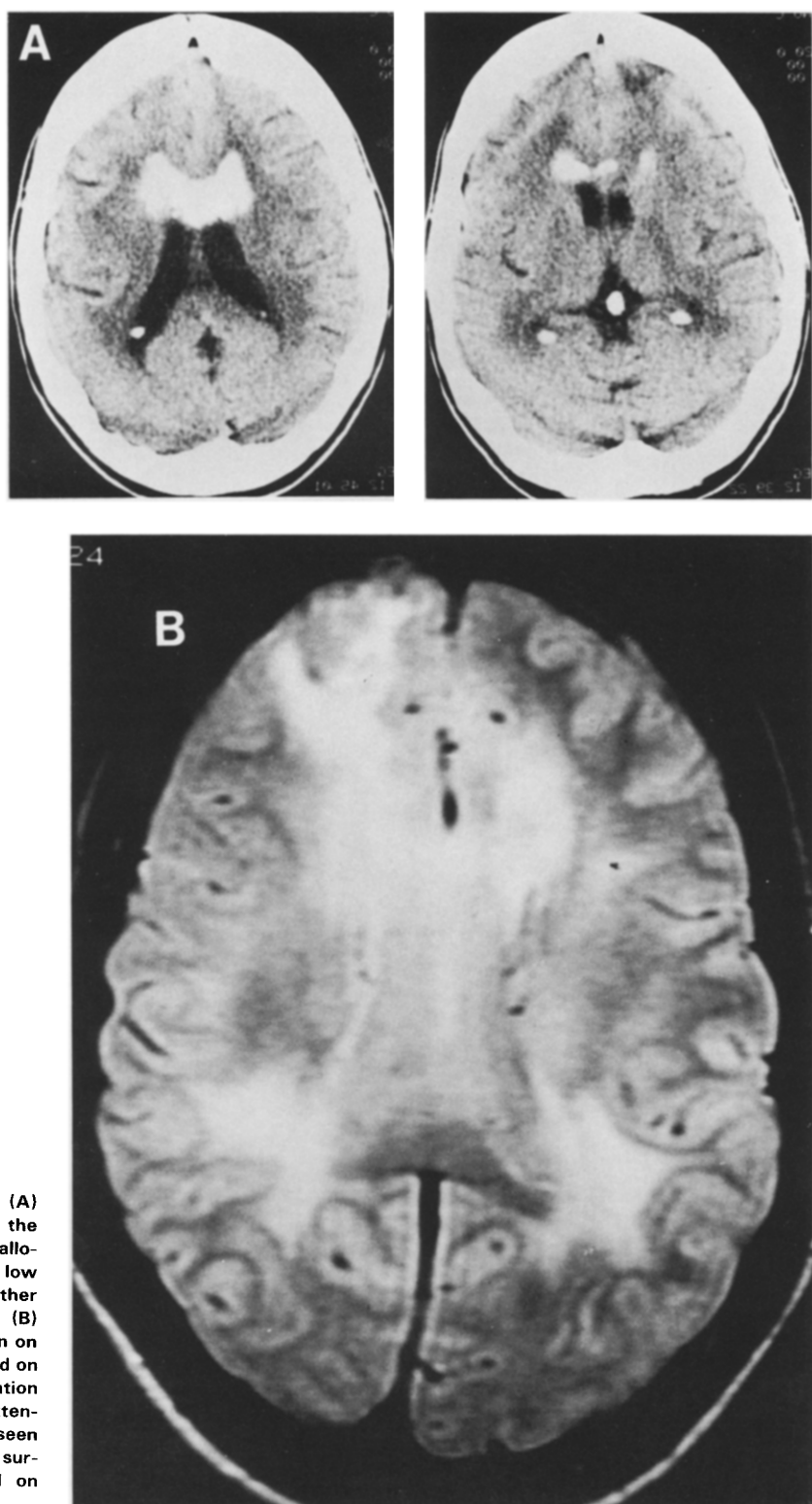


Fig 15. Low-grade tumor. (A) XCT: An area of calcification in the anterior aspect of the corpus callosum. This is consistent with a low grade tumor in this location. No other abnormality is seen elsewhere. (B) MRI: the area of calcification seen on the XCT scans cannot be detected on this image. This is a known limitation of the MR imaging. However, extensive white matter abnormality is seen that is probably due to edema surrounding the tumor. (continued on page 28.)

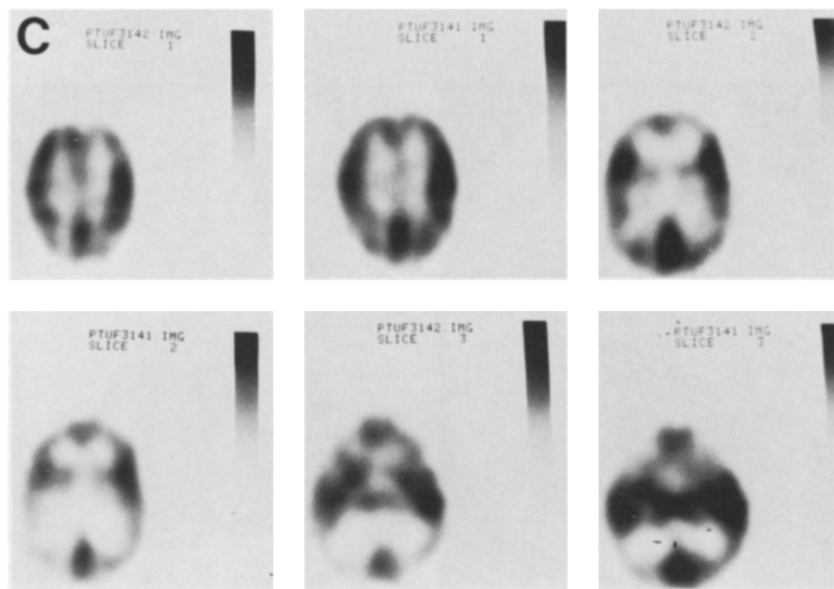


Fig 15. (cont'd) (C) PET: the PET scans except for minimal decreased metabolic activity in the basal ganglia region are within normal limits. The area of the tumor cannot be clearly defined on the metabolic scan.

MRI with powerful magnets (especially with MR contrast agents) may prove superior to XCT imaging. As discussed previously, on the PET scans the low-grade tumors reveal hypometabolism, while grade 3 and 4 gliomas show hypermetabolism compared with the surrounding brain. Areas of decreased metabolism were noted adjacent to and remote from the tumor on PET images. These areas appeared normal on XCT and MR scans.

We recently studied several patients with intracranial bleeding secondary to head trauma. In the acute stage of head injury, MRI was superior to XCT in identification and the precise location of hemorrhage and associated edema. Small cerebral hematomas diagnosed by MRI were missed with XCT. The extent of apparent encephalomalacia in the chronic stages of injury also was better defined with MRI. In these patients PET scans (FDG) detected hypometabolic areas of brain dysfunction, which were not visualized by XCT or MRI (Fig 17). In addition, every structural lesion detected by anatomic scanning, except for the small brain hemorrhages seen on MRI, was accompanied by a reduction of metabolism in the appropriate region. Particularly striking was reduced metabolism in both anterior temporal lobes with sparing of the posterior temporal lobes in all patients scanned during the acute posttrauma period. In two patients

metabolism remained significantly reduced in the ostensibly normal lobe at 6 months.

In patients with senile dementia, MR and XCT scans showed ventricular dilatation and cortical atrophy, although the latter appeared more pronounced on MRI studies. With normal aging some changes (increased T2 signal intensity) were noted periventricularly on MRI scans with no corresponding XCT abnormalities. The histologic correlate of this finding remains unclear. Old infarcts that may cause MID are more frequently and distinctly seen on the MR than XCT scans. Patients with psychiatric and seizure disorders mostly appeared within normal limits on XCT and MR scans, while PET scans revealed certain abnormalities as described above. Our early data indicate that MRI is superior to XCT in detecting acute infarcts. However, the FDG technique is more sensitive than both in the early detection of acute cerebral infarcts.

This preliminary investigation indicates that MRI provides excellent delineation of structural abnormalities in the brain. This is achieved without the administration of iodine-based contrast-enhancing agents or exposure to ionizing radiation. Because of these advantages, MRI will continue to be refined and its role in the diagnosis of CNS disorders further explored. MRI may prove to be superior to XCT in the evaluation of

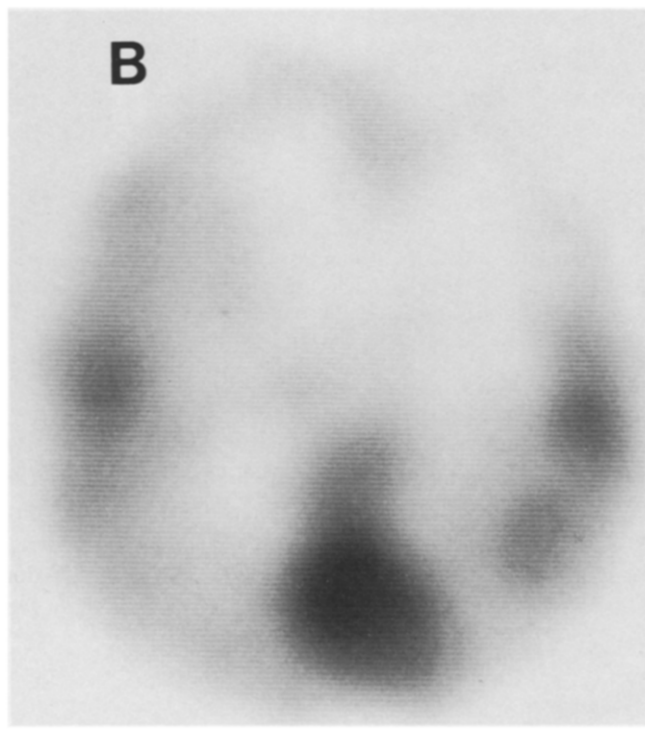
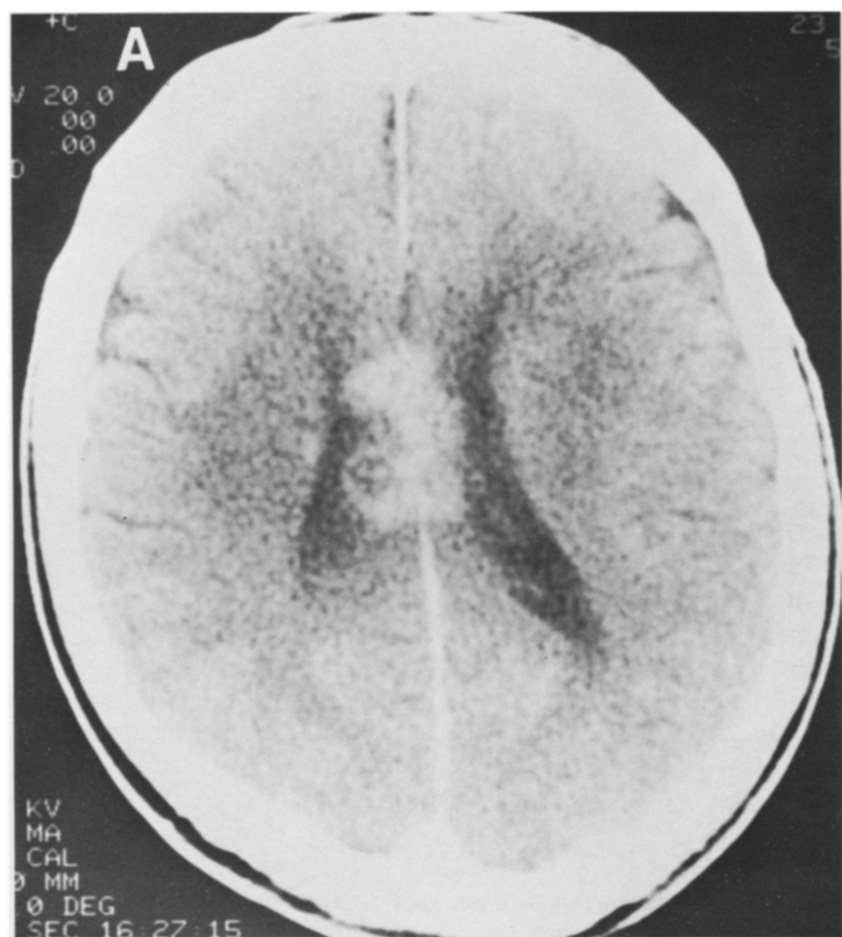


Fig 16. Postradiation necrosis. (A) PET: an area of intense contrast enhancement is seen in the corpus callosum in a patient who had cranial radiation several months earlier. This was interpreted to be consistent with a primary brain tumor. However, other possibilities such as necrosis were not ruled out. A surgical biopsy revealed necrotic tissue at this site. T1 weighted MR images were within normal limits. (B) PET: An FDG scan at the level of corpus callosum demonstrates a normal pattern at the site of XCT abnormality. This combination is most consistent with radiation induced necrosis at this site. Decreased metabolism in the right frontal lobe is probably due to edema in this lobe.

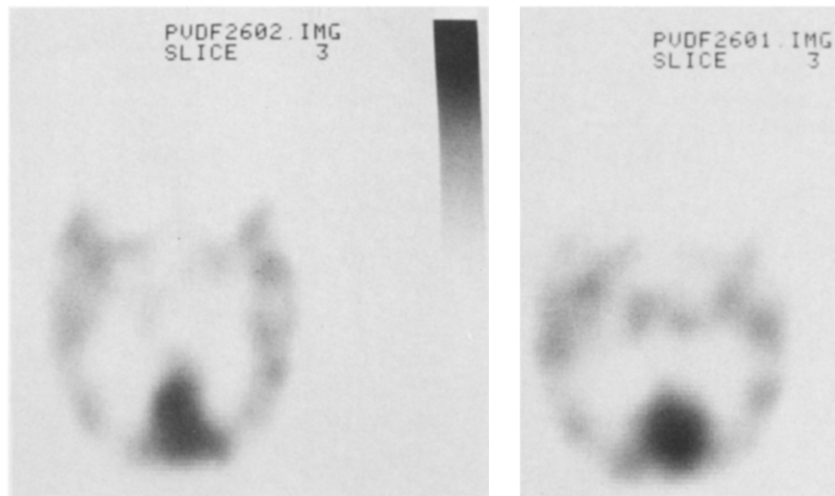


Fig 17. Head trauma. In this patient with head injury, significant hypometabolism is noted in both frontal lobes. Corresponding XCT and MR images appeared within normal limits.

certain disorders such as cerebral ischemia, head injury, brain tumors, and white matter lesions.

PET imaging, on the other hand, demonstrates regional function and metabolism, albeit with less detailed resolution than obtained by either XCT or MRI. This metabolic information may

be crucial in the management of patients without structural cerebral abnormalities. PET studies, therefore, will continue to play a major complementary role to anatomic scanning in managing and understanding CNS disorders.

REFERENCES

1. Sokoloff L, Reivich M, Kennedy C, DesRosier M, Patlak C, Pettigrew D, Sakurada G, Shinohara M: The [^{14}C]deoxyglucose method for the measurement of local cerebral glucose utilization: Theory, procedure and normal values in the conscious and anesthetized albino rat. *J Neurochem* 28:897-916, 1977
2. Bidder TG: Hexose translocation across the blood-brain interface: Configurational aspects. *J Neurochem* 15:867-874, 1968
3. Sols A, Crane RK: Substrate specificity of brain hexokinase. *J Biol Chem* 210:581-595, 1954
4. Reivich M, Kuhl DE, Wolf A, Greenberg J, Phelps M, Ido T, Casella V, Fowler J, Alavi A, Som P, Sokoloff L: The [^{18}F]-fluorodeoxyglucose method for the measurement of local cerebral glucose utilization in man. *Circ Res* 44:127-137, 1979
5. Phelps ME, Huang SC, Hoffman EJ, Selin C, Sokoloff L, Kuhl DE: Tomographic measurement of local cerebral glucose metabolic rate in humans with ($\text{F}-18$) 2-fluoro-2-deoxy-D-glucose. Validation of method. *Ann Neurol* 6:371-388, 1979
6. Huang SC, Phelps ME, Hoffman EJ, Sideris K, Selin CJ, Kuhl DE: Noninvasive determination of local cerebral metabolic rate of glucose in man. *Am J Physiol* 238:E69-E82, 1980
7. Alavi A, Reivich M, Jones SC: Functional imaging of the brain with positron emission tomography, in Weissman HS, Freeman LM (eds): *Nuclear Medicine Annual* 1982. New York, Raven, 1982, pp 319-372
8. Phelps ME, Mazziotta JC, Huang S-C: Study of cerebral function with positron computed tomography. *J Cereb Blood Flow Metab* 2:113-162, 1982
9. Phelps ME, Hoffman EJ, Mullani NA, Ter-Pogossian MM: Transaxial emission reconstruction tomography: Coincidence detection of positron emitting radionuclides, in DeBlanc H, Sorenson JA (eds): *Noninvasive Brain Imaging, Radionuclides and Computed Tomography*. New York, Society of Nuclear Medicine, 1975, pp 87-109
10. Reivich M, Alavi A, Wolf A, Fowler J, Russell J, Arnett C, MacGregor RR, Shiu CY, Atkins H, Anand A, Dann R, Greenberg J: Glucose metabolic rate kinetic model parameter determination in humans: The lumped constants and rate constants for [^{18}F]fluorodeoxyglucose and [^{11}C]deoxyglucose. *J Cereb Blood Flow Metab* 5:179-192, 1985
11. Heiss W-D, Pawlik G, Herholz K, Wagner R, Goldner H, Weinhard K: Regional kinetic constants and cerebral metabolic rate for glucose in normal human volunteers determined by dynamic positron emission tomography of [^{18}F]-2-fluoro-2-deoxy-D-glucose. *J Cereb Blood Flow Metab* 4:212-223, 1984
12. Hawkins RA, Phelps ME, Huang SC, Kuhl DE: Effect of ischemia on quantification of local cerebral glucose metabolic rate in man. *J Cereb Blood Flow Metab* 1:37-51, 1981
13. Hawkins RA, Mazziotta JC, Phelps ME, Huang SC, Kuhl DE, Carson RE, Metter EJ, Riege WH: Cerebral glucose metabolism as a function of age in man: Influence of the rate constants in the fluorodeoxyglucose method. *J Cereb Blood Flow Metab* 3:250-253, 1983
14. Crane PD, Pardridge WM, Braum LD, Oldendorf WH: Kinetics of transport and phosphorylation of 2-fluoro-2-deoxy-D-glucose in rat brain. *J Neurochem* 40:160-167, 1979

15. Gjedde A, Wienhard K, Heiss W-D, Kloster G, Diemer NH, Herholz K, Pawlik G: Comparative regional analysis of 2-fluorodeoxyglucose and methylglucose uptake in brain of four stroke patients. With special reference to the regional estimation of the lumped constant. *J Cereb Blood Flow Metab* 5:163–178, 1985
16. Hoffman EJ, Huang SC, Phelps ME: Quantitation in positron emission tomography. 1. Effect of object size. *J Comput Assist Tomogr* 3:299–308, 1979
17. Huang SC, Hoffman EJ, Phelps ME, Kuhl DE: Quantitation in positron emission computed tomography. 2. Effect of inaccurate attenuation correction. *J Comput Assist Tomogr* 3:804–814, 1979
18. Huang SC, Hoffman EJ, Phelps ME, Kuhl DE: Quantitation in positron emission computed tomography. 3. Effect of sampling. *J Comput Assist Tomogr* 4:819–826, 1980
19. Hoffman EJ, Huang SC, Phelps ME, Kuhl DE: Quantitation in positron emission tomography. 4. Effect of accidental coincidences. *J Comput Assist Tomogr* 5:391–400, 1981
20. Hoffman EJ, Huang SC, Plummer D, Phelps ME: Quantitation in positron emission computed tomography. 6. Effect of nonuniform resolution. *J Comput Assist Tomogr* 6:987–999, 1982
21. Mazziotta JC, Phelps ME, Plummer D, Kuhl DE: Quantitation in positron emission computed tomography. 5. Physical-anatomical effects. *J Comput Assist Tomogr* 5:734–743, 1981
22. Huang SC, Phelps ME, Hoffman EJ, Kuhl DE: Error sensitivity analysis of fluorodeoxyglucose method for measurement of cerebral metabolic rate of glucose. *J Cereb Blood Flow Metab* 1:391–401, 1981
23. Hoffman EJ, van der Stee M, Ricci AR, Phelps ME: Prospects for both precision and accuracy in positron emission tomography. *Ann Neurol* 15:S25–S34, 1984 (suppl)
24. Braak H: Studies of brain function 4. Architectonics of the human telencephalic cortex. New York, Springer-Verlag, 1980
25. Diamond IT: The subdivisions of neocortex: A proposal to revise the traditional view of sensory, motor, and association areas. *Prog Psychobiol Physiol Psychol* 8:1–43, 1979
26. Merzenich MM, Kaas JH: Principles of organization of sensory-perceptual systems in mammals. *Prog Psychobiol Physiol Psychol* 9:1–41, 1980
27. Greenberg JH, Reivich M, Alavi A, Hand P, Rosenquist A, Rintelmann W, Stein A, Tusa R, Dann R, Christman D, Fowler J, MacGregor B, Wolf A: Metabolic mapping of functional activity in man with 18F-fluoro-deoxyglucose technique. *Science* 212:678–680, 1981
28. Mazziotta JC, Phelps ME, Carson RE, Kuhl DE: Tomographic mapping of human cerebral metabolism: Sensory deprivation. *Ann Neurol* 12:435–444, 1982
29. Mazziotta JC, Phelps ME, Miller J, Kuhl DE: Tomographic mapping of human cerebral metabolism. Normal unstimulated state. *Neurology* 31:503–516, 1981
30. Finklestein S, Alpert NM, Ackerman RH, Correia JA, Buonanno FS, Chang J, Brownell GL, Taveras JM: Positron brain imaging—Normal patterns and asymmetries. *Brain Cognition* 1:286–293, 1982
31. Sarkisov SA: The Structure and Functions of the Brain, N. Raskin (ed). Bloomington, Ind, Indiana University Press, 1966
32. Stensass SS, Eddington DK, Dobelle WH: The topography and variability of the primary visual cortex in man. *J Neurosurg* 40:747–755, 1974
33. Reivich M, Alavi A, Greenberg JH, Fowler J, Christman D, MacGregor R, Jones SC, London J, Shiue C, Yonekura Y: Use of 2-deoxy-d-[1-¹¹C]glucose for the determination of local cerebral glucose metabolism in humans: Variation within and between subjects. *J Cereb Blood Flow Metab* 2:307–319, 1982
34. Chang J, Duara R, Barker W, Apicella A, Gilson A: A strategy for obtaining both resting and psychologically activated state metabolic data from a single PET study using [F-18]-fluorodeoxyglucose (FDG). *J Nucl Med* 26:P103, 1985
35. Brooks G, Di Chiro G, Zukerberg B, Bairamian D, Larson S: Test-retest studies of glucose metabolic rate with F-18-deoxyglucose. *J Nucl Med* 26:P68, 1985.
36. Phelps ME, Hoffman EJ, Mullani NA, Higgins CS: Design considerations for a whole body positron emission transaxial tomograph (PETT III). *IEEE Nucl Sci NS* 23:516–522, 1976
37. Alavi A, Reivich M, Greenberg J, Christman D, Fowler J, Hand P, Rosenquist A, Rintelmann W, and Wolf A: Mapping of functional activity in brain with 18-F-fluoro-deoxyglucose. *Semin Nucl Med* 11:24–31, 1981
38. Phelps ME, Hoffman EJ, Huang SC, Kuhl DE: ECAT: A new computerized tomographic imaging system for positron emitting radiopharmaceuticals. *J Nucl Med* 19:635, 1978 (abstr)
39. Phelps ME, Mazziotta JC: Positron emission tomography: Human brain function and biochemistry. *Science* 228:799–809, 1985
40. Geschwind N, Levitsky W: Human brain: Left-right asymmetries in temporal speech region. *Science* 161:186–187, 1968
41. Whitaker HA, Selnes OA: Anatomic variations in the cortex: Individual differences and the problem of the localization of language functions. *Ann NY Acad Sci* 280:844–854, 1976
42. Kushner M, Schwartz R, Alavi A, Dann R, Rosen M, Silver F, Reivich M: Cerebral activation by nonmeaningful monaural verbal auditory stimulation. (manuscript in preparation)
43. Mazziotta JC, Phelps ME, Carson RE, Kuhl DE: Tomographic mapping of human cerebral metabolism. Auditory stimulation. *Neurology* 32:921–928, 1982
44. Tusa RJ, Palmer LA, Rosenquist AC: Multiple cortical visual areas: Visual field topography in the cat, in Woolsey CN (ed): *Cortical Sensory Organization*, Vol 2. New Jersey, Humana, 1981, pp 1–31
45. Allman JM, Baker JF, Newsome WT, Petersen SE: Visual topography and function: Cortical visual areas in the owl monkey, in Woolsey CN (ed): *Cortical Sensory Organization*, Vol 2. New Jersey, Humana, 1981, pp 171–185
46. Gross CG, Bruce CJ, Desimone R, Fleming J, Gattass R: Cortical visual areas of the temporal lobe: Three areas in the Macaque, in Woolsey CN (ed): *Cortical Sensory Organization*, Vol 2. New Jersey, Humana, 1981, pp 187–216

47. Phelps ME, Kuhl DE, Mazziotta JC: Metabolic mapping of the brain's response to visual stimulation: Studies in man. *Science* 211:1445-1448, 1981
48. Ter-Pogossian MM, Mullani NA, Hood J: Design considerations for a positron emission tomograph (PETT V) for imaging of the brain. *J Comput Assist Tomogr* 2:539-544, 1978
49. Kushner M, Rosenquist A, Alavi A, Dann R, Burke A, Greenberg J, Reivich M: Visual areas of the human brain: A positron emission tomographic study. (submitted for publication)
50. Fox PT, Raichle ME: Stimulus rate dependence of regional cerebral blood flow in human striate cortex, demonstrated by positron emission tomography. *J Neurophysiol* 51:1109-1120, 1984
51. Bosley TM, Dann R, Silver F, Alavi A, Kushner M, Sergott R, Savino PJ, Schatz NJ, Reivich M: Lesions of the optic chiasm: Positron emission tomography. (submitted for publication)
52. Bosley TM, Rosenquist AC, Kushner M, Burke A, Stein A, Dann R, Cobbs W, Savino PJ, Schatz NJ, Alavi A, Reivich M: Ischemic lesions of the occipital cortex and optic radiations: Positron emission tomography. *Neurology* 35:470-484, 1985
53. Phelps ME, Mazziotta JC, Kuhl DE, Nuwer M, Packwood J, Metter J, Engel J Jr: Tomographic mapping of human cerebral metabolism: Visual stimulation and deprivation. *Neurology* 31:517-529, 1981
54. Dann R, Muehllehner G, Rosenquist A: Computer aided data analysis of ECT data. *J Nucl Med* 24:82, 1983
55. Mazziotta JC, Phelps ME, Meadors AK, Ricci A, Winter J, Bentson JR: Anatomical localization schemes for use in positron computed tomography using a specially designed headholder. *J Comput Assist Tomogr* 6:858-853, 1982
56. Fox PT, Perlmuter JS, Raichle ME: A stereotactic method of anatomical localization for positron emission tomography. *J Comput Assist Tomogr* 9:141-153, 1985
57. Dann R, Muehllehner G: Computer-assisted analysis of brain ECT data. (submitted for publication)
58. Herholz K, Pawlik G, Wienhard K, Heiss W-D: Computer assisted mapping in quantitative analysis of cerebral positron emission tomography. *J Cereb Blood Flow Metab* 9:154-161, 1985
59. Bajcsy R, Lieberson R, Reivich M: A computerized system for the elastic matching of deformed radiographic images to idealized atlas imaging. *J Comput Assist Tomogr* 7:618-625, 1983
60. Bohm C, Greitz T, Kingsley D, Olsson L: The construction of a computerized individually adjustable stereotaxic brain atlas for use in neurosurgery and PET studies, in Raynaud C (ed): Nuclear Medicine and Biology II. Paris, Pergamon, 1982, pp 2011-2013
61. Mazziotta JC: Physiologic neuroanatomy: New brain imaging methods present a challenge to an old discipline. *J Cereb Blood Flow Metab* 4:481-483, 1984 (editorial)
62. Duara R: Brain region localization in positron emission tomographic images. *J Cereb Blood Flow Metab* 5:343-345, 1985 (letter)
63. Metter EJ, Riege WH, Kuhl DE, Phelps ME: Cerebral metabolic relationships for selected brain regions in healthy adults. *J Cereb Blood Flow Metab* 4:1-7, 1984
64. Horwitz B, Duara R, Rapoport SI: Intercorrelations of glucose metabolic rates between brain regions: Application to healthy males in a state of reduced sensory input. *J Cereb Blood Flow Metab* 4:484-499, 1984
65. Phelps ME, Chugani H: Human brain development in infants with PET and FDG. *J Nucl Med* 26:P46, 1985 (abstr)
66. Kuhl DE, Metter EJ, Riege WH, Phelps ME: Effects of human aging on patterns of local cerebral glucose utilization determined by the [18F] fluorodeoxyglucose method. *J Cereb Blood Flow Metab* 2:163-171, 1982
67. Alavi A, Ferris S, Wolf A, Reivich M, Farkas T, Dann R, Christman D, Fowler J: Determination of cerebral metabolism in senile dementia using F-18-deoxyglucose and positron emission tomography. *J Nucl Med* 21:21, 1980 (abstr)
68. Alavi A, Ferris S, Wolf A, Christman D, Fowler J, MacGregor R, Farkas T, Greenberg J, Dann R, Reivich M: Determination of regional cerebral metabolism in dementia using F-18 deoxyglucose and positron emission tomography. Satellite Symposium on Physiological and Pathophysiological Aspects of Aging Brain: Experimental Brain Research. Heidelberg, Springer-Verlag, 1981
69. Ferris SH, DeLeon MS, Wolf AP, Farkas T, Christman DR, Reisberg B, Fowler JS, MacGregor R, Goldman A, George AE, Rampal S: Positron emission tomography in the study of aging and senile dementia. *Neurobiol Aging* 1:127-131, 1981
70. Ferris SH, DeLeon MJ, Wolf AP, George AE, Reisberg B, Christman DR, Yonekura Y, Fowler JS: Positron emission tomography in dementia, in Mayeux R, Rosen WG (eds): The Dementias. New York, Raven, 1983, pp 123-129
71. DeLeon MJ, Ferris SH, George AE, Christman DR, Fowler JS, Gentes C, Reisberg B, Gee B, Emmerich M, Yonekura Y, Brodie J, Kricheff TI, Wolf AP: Positron emission tomographic studies of aging and Alzheimer disease. *AJR* 4:568-571, 1983
72. Rapoport SI, Duara R, Horasitz B, Kessler RM, Sokoloff L, Ingvar DH, Grady C, Cutler N: Brain aging in 40 healthy men: rCMRglu and correlated functional activity in various brain regions in the resting state. *J Cereb Blood Flow Metab* 3:5454-5485, 1983 (suppl 1)
73. DeLeon MJ, George AE, Ferris SH, Christman DR, Fowler JS, Gentes CI, Brodie J, Reisberg B, Wolf AP: Positron emission tomography and computerized tomography of the aging brain. *J Comput Tomogr* 8:88-94, 1984
74. Alavi A, Chawluk J, Leonard J, Zimmerman R, Reivich M: Correlative imaging of the brain in aging and dementia with positron emission tomography, x-ray computed tomography and magnetic resonance imaging. Proceedings of the WHO Symposium on Mental Health Research in the Elderly—Present and Future Prospects, Mannheim, Sept 10-14, 1984. Hafner H, Moschel G, and Sartorius N (eds): Heidelberg-New York, Springer-Verlag, 1985 (in press)
75. Alavi A, Chawluk J, Hurtig H, Dann R, Rosen M, Kushner M, Silver F, Reivich M: Determination of patterns of regional cerebral glucose metabolism in normal aging and dementia. *J Nucl Med* 26:P69, 1985 (abstr)
76. Chawluk J, Alavi A, Hurtig H, Dann R, Rosen M,

- Kushner MJ, Silver FL, Reivich M: Altered patterns of regional cerebral glucose metabolism in aging and dementia. *J Cereb Blood Flow Metab* 1985 (in press) (suppl) (abstr)
77. Frackowiak RSJ, Pozzilli C, Legg NJ, DuBoulay GH, Marshall J, Lenzi GL, Jones T: Regional cerebral oxygen supply and utilization in dementia. *Brain* 104:753–778, 1981
 78. Foster NL, Chase TN, Fedio P, Patronas NJ, Brooks RA, DiChiro G: Alzheimer's disease: Focal cortical changes shown by PET. *Neurology* 33:961–965, 1983
 79. Chase TN, Foster NL, Fedio P, Brooks R, Mansi L, DiChiro G: Regional cortical dysfunction in Alzheimer's disease as determined by positron emission tomography. *Ann Neurol* 15:S170–174, 1984 (suppl 1)
 80. Friedland RP, Budinger TF, Ganz E, Yano Y, Mathis CA, Koss B, Ober BA, Huesman RH, Derenzin SE: Regional cerebral metabolic alterations in dementia of the Alzheimer type: Positron emission tomography with [18F] fluorodeoxyglucose. *J Comput Tomogr* 7:590–598, 1983
 81. Alavi A, Leonard JC, Chawluk J, Zimmerman RA, Dann RW, Alavi A, Edelstein W, Bottomley P, Redington R, Reivich M: Correlative studies of the brain with positron emission tomography, nuclear magnetic resonance, and x-ray computed tomography. In Hartmann A, Hoyer S (eds): *Cerebral Blood Flow and Metabolism Measurement*. Heidelberg, Springer-Verlag, 1985, pp 523–534
 82. Chawluk J, Alavi A, Dann R, Kushner MN, Hurtig H, Zimmerman RA, Reivich M: PET measurements of cerebral metabolism corrected for CSF contributions. *J Nucl Med* 25:56–57, 1984
 83. Kuhl DE, Metter EJ, Riege WH: Patterns of local cerebral glucose utilization determined in Parkinson's disease by the [18F] fluorodeoxyglucose method. *Ann Neurol* 15:419–424, 1984
 84. Kuhl DE, Metter EJ, Benson DF, Ashford JW, Riege WH, Fujikawa DG, Markham CH, Maltese A, Dorsey DA: Similarities of cerebral glucose metabolism in Alzheimer's and parkinsonian dementia. *J Nucl Med* 26:P69, 1985 (abstr)
 85. Kuhl DE, Phelps ME, Markham CH, Metter EJ, Riege WH, Winter J: Cerebral metabolism and atrophy in Huntington's disease determined by FDG and CT scan. *Ann Neurol* 12:425–434, 1982
 86. Phelps ME, Mazziotta JC, Wapenski J, Riege W, Baxter LR: Cerebral glucose utilization and blood flow in Huntington's disease. *J Nucl Med* 26:P47, 1985 (abstr)
 87. Ackerman RH, Alpert NM, Correia JA, Grotta JC, Fallick JT, Chang JY, Brownell GL, Taveras JM: Correlations of positron emission scans with TCT scans and clinical course. *Acta Neurol Scand* 60:230–231, 1979 (suppl 72)
 88. Kuhl DE, Phelps ME, Kowell AP, Metter EJ, Selin C: Effects of stroke on local cerebral metabolism and perfusion: Mapping by emission computed tomography of ¹⁸FDG and ¹³NH₃. *Ann Neurol* 8:47–60, 1980
 89. Kushner M, Reivich M, Alavi A, Silver F, Burke A, Dann R: Local and remote metabolic disturbances following acute cerebral infarction. *Neurology* 34:116, 1984 (suppl 1) (abstr)
 90. Lassen NA: The luxury perfusion syndrome and its possible relation to acute metabolic acidosis localized within the brain. *Lancet* 2:1113–1115, 1966
 91. Baron JC, Bousser MG, Comar D, Soussaline F, Castaigne P: Noninvasive tomographic study of cerebral blood flow and oxygen metabolism in vivo. *Eur Neurol* 20:273–284, 1981
 92. Lenzi GL, Frackowiak RSJ, Jones T: Regional cerebral blood flow (CBF), oxygen utilization (CMRO₂) and oxygen extraction ratio (OER) in acute hemispheric stroke. *J Cereb Blood Flow Metab* 1:S504–505, 1981 (suppl 1)
 93. Baron JC, Rougemont D, Bousser MG, Lebrun-Grandjean P, Iba-Zizen TM: Local CBF, oxygen extraction fraction (OEF), and CMRO₂: Prognostic value in recent supratentorial infarction in humans. *J Cereb Blood Flow Metab* 3:S1–S2, 1983 (suppl)
 94. Lenzi GL, Frackowiak RSJ, Jones T: Cerebral oxygen metabolism and blood flow in human cerebral ischemic infarction. *J Cereb Blood Flow Metab* 2:321–335, 1982
 95. Lebrun-Grandjean P, Baron J, Soussaline F, Loch'h C, Sastre J, Bousser MG: Coupling between regional blood flow and oxygen utilization in the normal human brain: A study with positron emission tomography and oxygen. *Arch Neurol* 40:230–236, 1983
 96. Reivich M: Blood flow metabolism couple in brain, in Plum F (ed): *Brain Dysfunction in Metabolic Disorders*. New York, Raven, 1974, pp 125–140
 97. Wise RJS, Rhodes CG, Gibbs JM, Hatazawa J, Palmer T, Frackowiak R: Disturbance of oxidative metabolism of glucose in recent human cerebral infarcts. *Ann Neurol* 14:627–637, 1983
 98. Baron JC, Rougemont D, Soussaline F, Bustany F, Crouzel C, Bousser MG: Local interrelationships of cerebral oxygen consumption and glucose utilization in normal subjects and in ischemic stroke patients: A positron emission tomography study. *J Cereb Blood Flow Metab* 4:140–149, 1984
 99. Syrota A, Castaing M, Rougemont D, Berridge M, Baron JC, Bousser MG: Tissue acid-base balance and oxygen metabolism in human cerebral infarction studied with positron emission tomography. *Ann Neurol* 14:419–428, 1983
 100. Lowry OH, Passonneau JV, Hassel FX, Schulz DW: Effect of ischemia on known substrates and cofactors of the glycolytic pathway in brain. *J Biol Chem* 239:18–30, 1963
 101. Gibbs JM, Wise RJS, Leenders KL, Jones T: Evaluation of cerebral perfusion reserve in patients with carotid-artery occlusion. *Lancet* 1(8372):310–314, 1984
 102. Powers JW, Grubb RL, Raichle ME: Physiological responses to focal cerebral ischemia in humans. *Ann Neurol* 16:546–552, 1984
 103. Baron JC, Bousser MG, Comar D, Duquesnoy JS, Castaigne P, Soussaline F, Castaigne P: Crossed cerebellar diaschisis: A remote functional depression secondary to supratentorial infarction of man. *J Cereb Blood Flow Metab* 1:S500–S501, 1981 (suppl 1)
 104. Kushner M, Alavi A, Reivich M, Dann R, Burke A, Robinson G: Contralateral cerebellar hypometabolism following cerebral insult: A positron emission tomography study. *Ann Neurol* 15:425–434, 1984
 105. Wise RJS, Bernardi S, Frackowiak RSJ, Legg NJ, Jones T: Serial observations on the pathophysiology of acute stroke: The transition from ischaemia to infarction as reflected in regional oxygen extraction. *Brain* 106:187–222, 1983
 106. Kempinsky WH: Experimental study of distant

- effects of acute focal brain injury. *Arch Neurol Psych* 79:376-389, 1958
107. Plum F, Howse DC, Duffy TE: Metabolic effects of seizures, in Plum F (ed): *Brain Dysfunction in Metabolic Disorders*, Vol 53. New York, Raven, 1974, pp 141-147
 108. Plum F, Posner JB, Tony B: Cerebral metabolic and circulation responses to induced convulsions in animals. *Arch Neurol* 18:1-13, 1968
 109. Engel J Jr: Functional localization of epileptogenic lesions. *Trends Neurosci* 6:60-65, 1983
 110. Alavi A, Leonard JC, Zimmerman RA, Dann RW, Chawluk J, Bottomley P, Redington R, Reivich M: Correlative studies of the brain with positron emission tomography (PET), nuclear magnetic resonance (NMR) and x-ray computed tomography (XCT). *J Nucl Med* 25:P9, 1984 (abstr)
 111. Engel J Jr, Kuhl DE, Phelps ME, Mazziotta JC: Interictal cerebral glucose metabolism in partial epilepsy and its relation to EEG changes. *Ann Neurol* 12:510-517, 1982
 112. Engel J Jr, Kuhl DE, Phelps ME, Crandall PH: Comparative localization of epileptic foci in partial epilepsy by PET and EEG. *Ann Neurol* 12:529-537, 1982
 113. Engel J Jr, Brown WJ, Kuhl DE, Phelps ME, Mazziotta JC, Crandall PH: Pathological findings underlying focal temporal lobe hypometabolism in partial epilepsy. *Ann Neurol* 12:518-528, 1982
 114. Engel J Jr, Rausch R, Lieb JP, Kuhl DE, Crandall PH: Correlation of criteria used for localizing epileptic foci in patients considered for surgical therapy of epilepsy. *Ann Neurol* 9:215-224, 1981
 115. Kuhl DE, Engel J Jr, Phelps ME, Selin C: Epileptic patterns of local cerebral metabolism and perfusion in humans determined by emission computed tomography of ¹⁸FDG and ¹³NH₃. *Ann Neurol* 8:348-360, 1980
 116. Engel J Jr, Kuhl DE, Phelps ME, Rausch R, Nuwer M: Local cerebral metabolism during partial seizures. *Neurology* 33:400-413, 1983
 117. Engel J Jr, Kuhl DE, Phelps ME: Patterns of human local cerebral glucose metabolism during epileptic seizures. *Science* 218:64-66, 1982
 118. Engel J Jr, Lubens P, Kuhl DE, Phelps ME: Local cerebral metabolic rate for glucose during petit mal absences. *Ann Neurol* 2:121-128, 1985
 119. Theodore WH, Newmark ME, Sato S, Brooks R, Patronas N, DeLaPaz R, DiChiro G, Kessler R, Margolin R, Manning RG, Channing M, Porter RJ: [18F] fluorodeoxyglucose positron emission computed tomography in refractory complex seizures. *Ann Neurol* 14:429-437, 1983
 120. Gur RC, Sussman NN, Alavi A, Gur RC, Rosen AD, O'Connor M, Greenberg J, Reivich M: Positron emission tomography in two cases of childhood epileptic encephalopathy (Lennox-Gastaut syndrome). *Neurology* 32:1191-1195, 1982
 121. DiChiro G, DeLaPaz RL, Brooks RA, Sokoloff L, Kornblith PL, Smith BH, Patronas NJ, Kufta CV, Kessler RM, Johnston GS, Manning RG, Wolf AP: Glucose utilization of cerebral gliomas measured by ¹⁵F) fluorodeoxyglucose and positron emission tomography. *Neurology* 32:1323-1329, 1982
 122. Patronas NJ, Brooks RA, DeLaPaz RL, Smith BH, Kornblith PL, DiChiro G: Glycolytic rate (PET) and contrast enhancement (CT) in human cerebral gliomas. *AJNR* 4:533-535, 1983
 123. Patronas NJ, DiChiro G, Smith BH, DeLaPaz RL, Brooks RA, Milam H, Kornblith PL: Depressed cerebellar glucose metabolism in supratentorial tumors. *Brain Res* 291:93-101, 1984
 124. DeLaPaz RL, Patronas NJ, Brooks RA, Smith BH, Kornblith PL, Milam H, DiChiro G: Positron emission tomographic study of suppression of gray matter glucose utilization by brain tumors. *AJNR* 4:826-829, 1983
 125. Patronas NJ, DiChiro G, Brooks RA, DeLaPaz RL, Kornblith PL, Smith BH, Rizzoli HV, Kessler RM, Manning RG, Channing M, Wolf AP, O'Connor CM: Work in Progress: (¹⁸F) fluorodeoxyglucose and positron emission tomography in the evaluation of radiation necrosis of the brain. *Radiology* 144:885-889, 1982
 126. Alavi J, Alavi A, Dann R, Kushner M, Chawluk J, Powlis W, Reivich M: Metabolic brain imaging correlated with clinical features and brain tumors. *J Nucl Med* 18:P64, 1985 (abstr)
 127. Patronas NJ, Di Chiro G, Kufta C, Bairamian D, Kornblith PL, Simon R, Larson S: Prediction of survival in glioma patients by means of positron emission tomography. *J Neurosurg* 62:816-822, 1985
 128. Buchsbaum MS, Ingvar DH, Kessler R, Waters RN, Capelletti J, van Kammen DP, King AC, Johnson JL, Manning RG, Flynn RW, Mann LS, Bunney WE, Sokoloff L: Cerebral glucography with positron emission tomography. *Arch Gen Psychiatry* 39:251-259, 1982
 129. Farkas T, Wolf AP, Jaeger J, Brodie JD, Christman DR, Fowler JS: Regional brain glucose metabolism schizophrenia. *Arch Gen Psychiatry* 41:293-300, 1984
 130. Wolkin A, Jaeger J, Brodie JD, Wolf AP, Fowler J, Rotrosen J, Gomez-Mont F, Cancro R: Persistence and cerebral metabolic abnormalities in chronic schizophrenia as determined by positron emission tomography. *Am J Psychiatry* 142:564-571, 1985
 131. Sheppard G, Manchanda R, Gruzelier J, Mirsch SR, Wise R, Frackowiak R, Jones T: ¹⁵O positron emission tomographic scanning in predominantly never treated acute schizophrenia patients. *Lancet* 1:1448-1452, 1983
 132. Phelps ME, Mazziotta JC, Baxter L, Gerner R: Positron emission tomographic study of affective disorders: Problems and strategies. *Ann Neurol* 15:S149-156, 1984 (suppl)
 133. Alavi A, Chawluk J, Leonard JC, Zimmerman RA, Alavi J, Dann RW, Edelstein W, Bottomley P, Redington R, Reivich M: Correlative studies of the brain positron emission tomography (PET), magnetic resonance imaging (MRI) and x-ray computed tomography (XCT). Presented at the XII International Symposium on Cerebral Blood Flow and Metabolism, June 16-20, 1985, Lund, Sweden, in Ingvar DH, Owman C, Siesjo BK (eds): *Proceedings of Brain 85*, New York, Raven, 1985 (in press)